UNIVERSITY OF BIRMINGHAM

EFFECTS OF FORMULATION AND PROCESSING CONDITIONS ON THE PHYSICAL PROPERTIES OF FAT CRYSTAL NETWORKS

by

BENYAMIN ASADIPOUR FARSANI

A thesis submitted to

The University of Birmingham

for the degree of

MASTER OF RESEARCH

School of Chemical Engineering

College of Engineering and Physical Sciences

The University of Birmingham

June 2013

ABSTRACT

Fats are employed in many industries and greatly contribute to the structure and texture of numerous food products, especially baked goods. Fats have high calorific values and dietary intake of high levels of fats (particularly saturated fats) has been linked to various health problems such as obesity, coronary heart disease, and some cancers. As a result of increasing demand for healthier, lower-fat products by consumers the food industry is seeking to produce low-fat and low-saturated fat products without affecting the desirable organoleptic properties dictated by the presence of fats.

This thesis investigates the effects of formulation and processing conditions on the material properties of fat crystal networks. A scraped surface heat exchanger was used to control crystallisation and to produce fat crystal networks. Experiments were conducted to study the effects of formulation (solid fat composition) and processing conditions (scraped surface heat exchanger's mixing speed, coolant temperature, and throughput).

Rheological studies were conducted to characterise the material properties of the fat systems. Viscosity measurements were carried out to study the effects of processing conditions on the material behaviour whilst oscillatory rheology was used to study the viscoelastic behaviour of the fat systems. Amplitude sweeps and oscillation tests (small scale rheological analysis) were conducted to study the viscous modulus (G'') and the elastic modulus (G') of the system which is an indicator of the macroscopic consistency of the network. Polarised light microscopy (PLM) was employed to observe the microstructure

of the crystallised system. These images were used alongside image analysis software, ImageJ, to quantify the complexity of the microstructural level of the fat crystal networks by calculating their box-counting fractal dimensions (D_b). The thermal behaviour of fat systems was studied using differential scanning calorimetry (DSC).

The results provide an insight into the effects of formulation and processing conditions on the physical properties of fat crystal networks. This allows the design of fat systems with specific behaviour by manipulating the processing conditions. The effect of formulation was investigated using a rapeseed oil/hydrogenated palm kernel oil system whilst the effect of processing was investigated on a rapeseed oil/tripalmitin system. It was found that the coolant temperature and the throughput of the crystallisation equipment (A-unit) inversely affect the values of viscosity, elastic modulus, and the viscous modulus of the fat systems produced. It was also shown that increasing the level of solid fat in the network directly affects and increases the viscosity, elastic modulus, viscous modulus, and the melting and crystallisation onset temperatures of the fat systems produced.

ACKNOWLEDGEMENTS

I would like to express my sincere gratitude to my supervisors at the University of Birmingham, Professor Ian T. Norton, Dr. Fotios Spyropoulos, and Dr. Thomas Mills for their advice and guidance throughout the course of this work. My gratitude also goes to Premier Foods and EPSRC for their financial support.

I am also grateful for the assistance provided by the staff at the department of Chemical Engineering in particular John Hooper, Lynn Draper, and Kathleen Hynes. I would also like to especially thank Dr. Richard Greenwood who continuously encouraged me throughout my time in the department.

My gratitude is also extended to all of my colleagues from the microstructure group who made my experience a pleasurable one. Special thanks to Amir Asghari, Aristodimos Lazidis, Marjan Rafiee, Ashkan Izadi, Nathan Burrill, Lucie Villedieu, Jonathan O'Sullivan, and Olga Mihailova for all of the good times.

A very special thank you goes to my dear friend Sam West for his unconditional support.

Most of all, I would like to thank my loving family; my father Foroud, my mother Eshrat, my brothers Danyal and Jorge, my sisters Felora and Farzaneh, my nephew Youhana, and last but not least, my favourite niece Tara.

TABLE OF CONTENTS

LIST OF FIGURES

1. INTRODUCTION

Food is an essential part of human existence; it is classed as a fundamental human need by Max-Neef *et al.* (1989), and is the basis of Maslow's hierarchy of needs (Maslow, 1943). Consumption of food provides us with the nutrients and calories needed for our well-being. Fat is an important part of a healthy diet as it is a great source of energy, and supplies essential fatty acids and fat-soluble vitamins. An estimated 80% of the total fat produced is used for food (Gunstone, 2006); this highlights the importance of fats in food products. Fats also hugely contribute to the desired texture of end products and help carry hydrophobic aroma compounds. Many fat-based food products require solid fats to interact with other ingredients in order to provide the desired structure and to offer oxidative stability (Sato, 2001b). Saturated fats are the only viable sources of the required high-melting (solid) fats as use of its alternative, *trans* fats, has been phased out or banned in some cases such as in Denmark, and New York City (Renton, 2010).

Over the past few decades dramatic changes have occurred in the eating habits of people living in the Western world. Technological advances over the past few decades have meant new ways of producing and marketing food have altered the eating behaviour of people. Fast food has become cheap and readily available, providing easy access to high-fat and high-calorie foods with ever increasing portion sizes. This alongside lower work-related physical activity has lead to a sedentary style of living, and has resulted in rising obesity rates; generally someone with a body mass index (BMI) of greater than 30 is considered obese.

The presence of excess dietary fat negatively impacts health due to the high calorific value of fat, which leads to obesity, and also because of the link between fats (particularly saturated fats) and other health issues.

The UK Health and Social Care Information Centre (HSCIC) reported that 24% of men and 26% of women in England were obese in 2011, which is an increase in obesity rates observed in 1993 when 13% and 16% of men and women respectively, were obese. In 2011/12, 9.5% of children aged 4-5 years and 19.2% of children aged 10-11 years were also classified as obese. The American Centres for Disease Control and Prevention state that in 2009/10 35.7% of adults and 17% of children in the United States were obese (Ogden *et al.*, 2012). This represented an increase in obesity rates across all population groups over the past several decades (CDC, 2011).

Obesity is not just an aesthetic issue as it leads to a number of serious health problems which are not only life threatening to the obese individual, but are also detrimental for the economy as a whole due to the huge costs involved in addressing and treating such conditions. Health problems related to being overweight or obese cost the UK's National Health Service (NHS) more than £5 billion per year (GOV.UK, 2013).

In the Saturated Fat and Energy Intake Programme published in 2008 by the UK Food Standards Agency (FSA) a reduction from 13.3% to below 11% in the average intake of saturated fat was recommended (FSA, 2008). This was because of the links between dietary saturated fat intake and various health issues such as blood cholesterol levels (both total and low-density lipoprotein, LDL), which in turn increase the risk of coronary heart disease (CHD). Saturated fats are also found to have links to other health issues as a meta-analysis carried out in 2001 found a statically significant relationship between the intake of saturated

fat and ovarian cancer (Huncharek and Kupelnick, 2001), while another carried out in 2003 illustrated a significant relationship between saturated fat intake and breast cancer (Boyd *et al.*, 2003). These are global issues and tackling them has resulted in a shift towards healthier lifestyles and therefore the need for products that address such health issues by containing less saturated fats.

A noteworthy proportion of the saturated fat intake is from baked products consumed as snacks; in the UK, a significant proportion (18%) of the saturated fat intake is from bakery and baked products (HMSO, 2002). With such health issues associated with saturated fats it is not surprising that the food industry seeks to reduce the amount of saturated fats through reformulation in many existing products or the formulation of totally new 'low-fat' or 'saturated fat-free' products.

In products such as cakes, solid fats stabilise the air cells which allows their expansion during heating; they also allow the occurrence of water retention and gluten hydration by providing a 'coating' layer for the flour (Talbot, 2011). The removal or replacement of these solid fats with softer fats, containing lower levels of saturated fatty acids, can negatively affect the quality of the end product through structural changes.

What the solid fat is replaced by is also very important. For instance a new meta-analysis has shown that replacing the saturated fats with polyunsaturated fats reduces the risk of CHD; but using carbohydrates as replacements increases the risk of 'non-fatal' CHD (Siri-Tarino *et al.*, 2010).

1.1. Objectives

The work done in this thesis is of industrial significance and the objectives that follow reflect on that. The long term objective of this thesis is to engineer bakery fats at a microstructural level to create a low-saturated fat ingredient that has the capability to be used to manufacture products with reduced-levels of saturated-fat, without compromising the quality characteristics of the existing products. In order to successfully achieve this objective it is required to understand the role of saturated fats in a fat system used to produce baked goods. This work investigates the effects of formulation and processing conditions on fat systems produced in a scraped surface heat exchanger, specifically the following parameters were studied:

- Viscosity
- Elastic and viscous moduli
- Melting and cooling behaviour
- Fractal dimension
- Thixotropy

1.2. Thesis Layout

The thesis structure is as follows. The introduction of the thesis is given in **Chapter 1**. A comprehensive literature review regarding fats and fat networks, rheological behaviour of fats, crystallisation, polymorphism, fractality and quantification of fractal networks was conducted and is reported in **Chapter 2**. The materials and techniques used and experimental procedures are described in **Chapter 3**.

Chapter 4 is devoted to the presentation of the results obtained from experiments studying the effects of solid fat concentration, scraper mixing speed, coolant temperature, and

throughput on the physical properties of fat systems produced in a scraped surface heat exchanger. **Chapter 5** summarises the findings and provides recommendations for enhancing the current study and also outlines recommendations for further investigations.

2. BACKGROUND AND THEORY

2.1. Fats and Oils

Fats and oils are present in many foods and are essential nutrients in both human and animal diets. They are great sources of energy, act as carriers of fat soluble vitamins, supply essential fatty acids, contribute to the feeling of satiety and render foods more pleasant. Meats, dairy products, poultry, fish and nuts are the main sources of fats and oils (ISEO, 1999).

Triglycerides (TAGs) are the major component of most food fats and oils; they are the result of the formation of one unit of glycerol with three units of fatty acids. The minor components of fats and oils include "monoglycerides, diglycerides, free fatty acids, phosphatides, sterols, fatty alcohols, fat soluble vitamins, and other substances". At room temperature they can range in form from liquid to solid; if liquid they are referred to as oils and if solid they are called fats. Factors which affect the physical characteristics of fats and oils include "the degree of unsaturation, the length of the carbon chains, the isomeric forms of the fatty acids, molecular configuration, and the type and extent of processing" (ISEO, 1999).

2.2. Fat Networks

Fat crystal networks are a particular class of soft materials, they exhibit yield stress and display viscoelastic properties, causing them to be labelled plastic (Narine and Marangoni, 1999b). The properties of food products containing significant amounts of fats, such as butter, chocolate and many spreads, are greatly affected by the macroscopic rheological properties of lipid networks; for instance many of the sensory attributes such as spreadability and mouthfeel are dependent on the mechanical strength of the underlying fat

crystal network (Narine and Marangoni, 1999b). Many researchers have focused on the physical properties of fats as certain textural properties are required for fat based products to meet desired sensory attributes, so as to achieve consumer acceptance (de Bruijne and Bot, 1999).

The macroscopic properties of a three-dimensional fat crystal network are affected by a number of factors. These are illustrated as a hierarchical model in Figure 2.1. The model suggests that lipid composition, processing conditions and storage conditions will affect the solid fat content (SFC), polymorphism and the morphology of the fat crystal network, which in turn affects the final macroscopic properties of the network (Martini *et al.*, 2006).

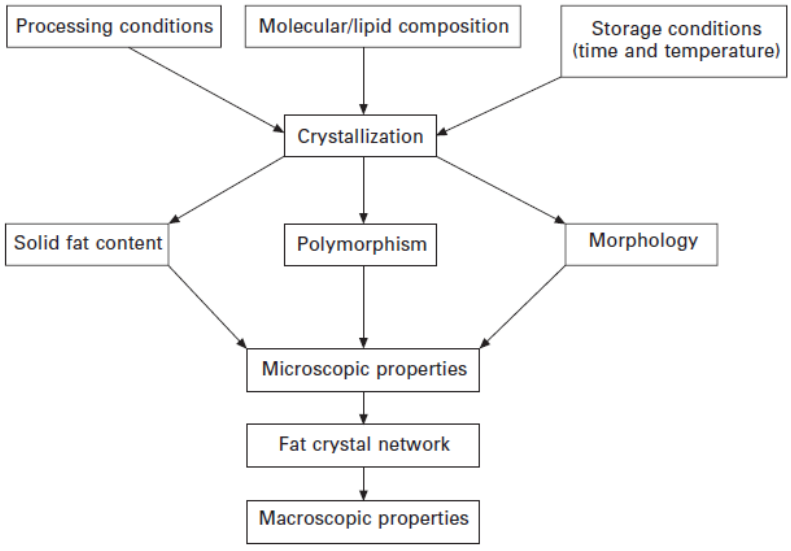

Figure 2.1: Hierarchical model for describing the formation and interaction of elements affecting the macroscopic properties of a three-dimensional fat crystal network (Martini et al., 2006).

The formation of structure of a typical fat network occurs as the fat crystallises from the melt. The triglycerides present in the sample crystallise into particular polymorphic phases, these crystals then grow into larger microstructural elements (~ 6 μm) which in turn aggregate via a mass- and heat-transfer limited process into larger microstructures (~ 100

μm) (Narine and Marangoni, 1999b). This is continued until a continuous three-dimensional network is formed through the aggregation of the microstructures, which trap the liquid phase within the network structure (Narine and Marangoni, 1999b, Martini *et al.*, 2006) . Narine and Marangoni (1999a) showed that the microstructural elements are arranged in a fractal manner within the microstructure. Figure 2.2 portrays the structural hierarchy of the organisation of a typical fat crystal network.

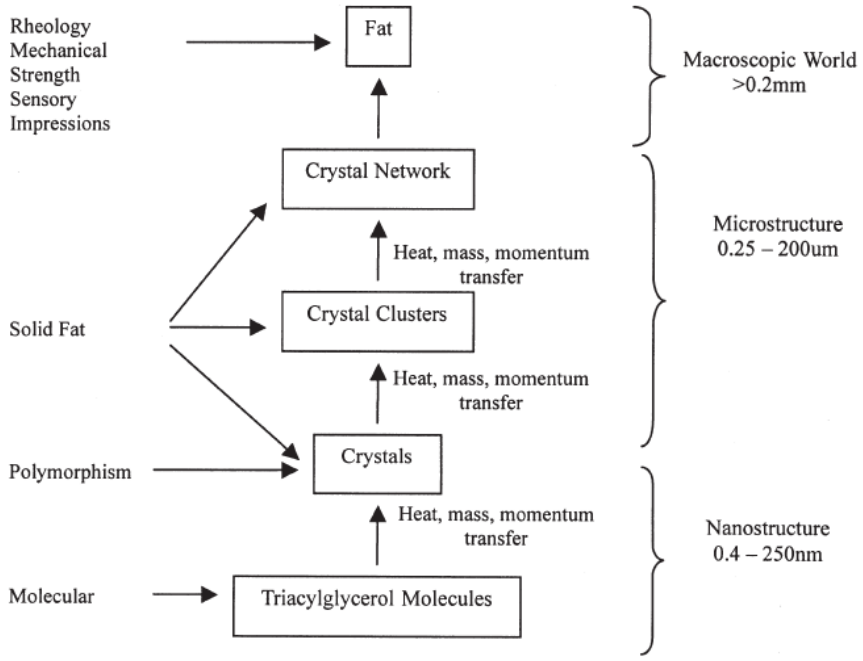

Figure 2.2: Microstructural hierarchy of fat crystal networks (Tang and Marangoni, 2006b)

The microstructural level of the fat crystal network may be defined as those structures in the length range between 0.25 and 200 μm. Crystallites may be observed at the lower range of the microstructural level, whilst at the upper ranges, aggregates of such elements (clusters of crystallites) are observed (Tang and Marangoni, 2006b). This level of structure greatly influences the macroscopic rheological properties of the fat network (Marangoni, 2002, deMan and Beers, 1987, Narine and Marangoni, 1999b).

Much work has been done in analysis of the microstructural level of the network, suggesting that consideration of this level of structure has huge importance in assessing the mechanical strength of the fat network, and the quantification of this level of structure has been achieved with the application of fractal mathematics to the geometry of the microstructure (Narine and Marangoni, 1999b). Fractal geometry has been proven to be helpful in characterisation of such complex systems (Narine and Marangoni, 1999a). The importance of the microstructural level of structural organisation becomes apparent when the different levels of structure in a fat network are examined in the context of how these levels of structure are responsible for the values of macroscopic physical measurements performed on the network (Narine and Marangoni, 1999b).

Many microscopy techniques have been used to visualise the microstructure of fat crystal networks and allow us to gain a deeper understanding of the structure of fat crystal networks. These methods include polarised light microscopy (PLM), scanning electron microscopy (SEM), confocal scanning light microscopy (CSLM), freeze-fracture electron microscopy (FFEM), and cryo-SEM. In addition to microscopy, large- and small-deformation rheology has been used to investigate the microstructure of fat crystal networks (Tang and Marangoni, 2006b). Penetrometry tests are also another method of measuring the mechanical properties of some fat systems (Gonzalez-Gutierrez and Scanlon, 2012).

2.2.1. Crystallisation

Nucleation is divided into two types, primary and secondary; with primary nucleation occurring where systems do not contain crystalline matter. Secondary nucleation refers to where nucleation occurs in the vicinity of crystals present in a supersaturated system (Mullin, 2001); this is illustrated in Figure 2.3. Primary nucleation is also separated into two types, homogeneous and heterogeneous nucleation. For homogeneous nucleation to take

place the molecules have to coagulate and become orientated into a fixed lattice (Mullin, 2001).

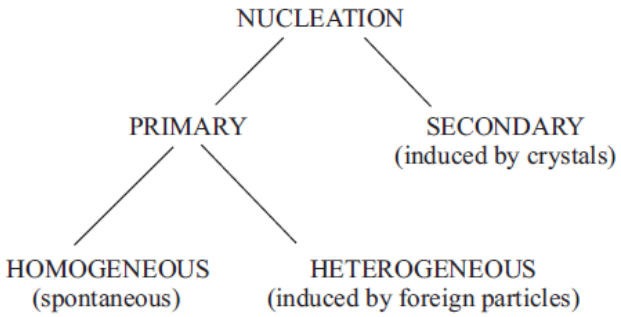

Figure 2.3: Nucleation schematic (Mullin, 2001).

Oils and fats are complex systems and are composed principally of combinations of triglycerides. Fats and oils contain different proportions of chemically distinct triglycerides made up of varying chain lengths and melting points; as a result a fat would melt over a range of temperatures instead of melting at a single temperature (Sangwal and Sato, 2012). The process of crystallisation of fats is further complicated due to the solubility of high melting glycerides in the lower melting glycerides, and also due to the polymorphic nature of triglycerides (Sangwal and Sato, 2012).

The driving force for crystallisation processes is the difference between the Gibbs free energy of the supersaturated or supercooled initial phase, G_I, and that of the newly forming phase, G_{II} (Sangwal and Sato, 2012). This can be expressed using Equation 2.1.

$$\Delta G = G_{II} - G_I = \Delta H - T\Delta S \qquad \text{Equation 2.1}$$

where H and S represent the enthalpy and entropy of a phase respectively, and $\Delta H = H_{II} - H_I$ and $\Delta S = S_{II} - S_I$ (Sangwal and Sato, 2012).

The formation of three-dimensional nuclei involves the ordered aggregation of atomic or molecular units. This process is generally thought of as occurring due to the collision of individual atoms or molecules, in a way that collision leads to increasing aggregate size (Sangwal and Sato, 2012). Some of these aggregates grow larger while others just disintegrate with time. However when the aggregates grow to a certain size, called the critical size, they no longer disintegrate with time; these nuclei are called three-dimensional stable nuclei (Sangwal and Sato, 2012). The critical size is the smallest size of a stable nucleus as it is only when the nucleus radius is greater than the critical radius that the free energy ΔG of formation of a nucleus decreases with increasing radius. It is normally assumed for the nuclei to prefer to obtain a rounded shape as a sphere has the lowest surface tension (Sangwal and Sato, 2012).

Homogeneous nucleation occurs in the absence of foreign sources; however this is not the case for most real systems as impurities in the materials, and also cracks and scratches on the surface of crystallisers act to catalyse the nucleation; this is referred to as heterogeneous nucleation (Sangwal and Sato, 2012).

Theoretically heterogeneous nucleation can be both two- or three-dimensional depending on the shape of the aggregates forming on the foreign substrate. For instance a cap shaped aggregate undergoes three-dimensional growth, whereas a disk shaped aggregate undergoes two-dimensional growth where its height remains unaltered (Sangwal and Sato, 2012). The surface properties and the size of foreign particles are important as they affect nucleation in different supersaturation regimes (Sangwal and Sato, 2012).

The microstructural properties of fat networks are greatly affected by the processing conditions of crystallisation (Heertje *et al.*, 1987, Heertje *et al.*, 1988, Herrera and Hartel,

2000, Martini *et al.*, 2006). Desirable polymorphic forms can be achieved through the application of shear and controlled cooling and so industrial manufacturing of fat systems involves shearing during the crystallisation process (Maleky and Marangoni, 2008).

Shearing during crystallisation is believed to improve the overall mixing of the system, and breaks up the newly formed crystallites around the seed crystals, thus increasing the number of seed crystals in the solution (Beckett, 2000, Stapley *et al.*, 1999). It is suggested that shearing during crystallisation affects the crystallisation kinetics and the crystal structure of polymorphic fat systems (Windhab, 1999). This is because the induction time is lowered with increasing shear rate (Bolliger *et al.*, 1998). It is also reported that more stable polymorphs are formed as a result of application of shear during crystallisation (MacMillan *et al.*, 2002). Shearing also introduces ordering in a fat crystal system (Maleky and Marangoni, 2008) as during crystallisation it aligns and moves the molecules of crystallite parallel to each other (Stapley *et al.*, 1999, Mazzanti *et al.*, 2003).

The rate of shear during crystallisation is also important as there is a critical shear rate that must be exceeded in order to produce seed crystals (Stapley *et al.*, 1999). At higher shear rates the solid fat crystals are broken and their fragments are uniformly distributed throughout the melt (Maleky and Marangoni, 2008), and so the degree of shearing is responsible for crystalline growth (Briggs and Wang, 2004).

2.2.2. Polymorphism

Polymorphism is where a solid compound exists in a number of crystalline forms, which have different physical properties (Britannica, 2013). Similar to other lipids, TAGs demonstrate complex polymorphism depending on environmental conditions as well as their thermal histories (Yano and Sato, 1999).

Tripalmitin (PPP), composed of three palmitic acid groups, has three polymorphic forms: *α*, *β'*, and *β* (Sato, 2001b) based on their subcell structure, Figure 2.4. The different polymorphic forms have different molecular structures: disordered aliphatic chain conformation in *α*, intermediate packing in *β'* and the most dense packing in the *β* form. Because of this the Gibbs free energy value is the highest in *α*, intermediate in *β'* and lowest in *β*; making the *β* polymorph the most stable (Sato, 2001b, Sangwal and Sato, 2012). It is thought that crystal morphology is affected by the molecular structures and the rate of crystallisation, and generally the crystal morphology for *α* is amorphous-like, for *β'* is 'tiny and bulky', and for *β* it is needle-like (Sato, 2001b).

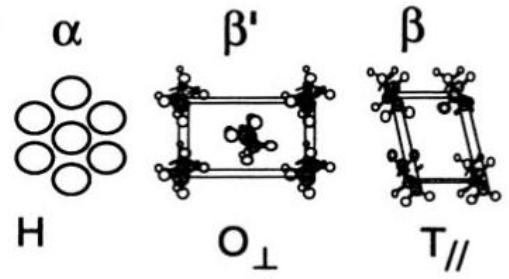

Figure 2.4: Subcell structures for different polymorphic forms (Sato, 2001a).

Polymorphic forms of a substance can also be characterised by differences in their enthalpies of melting ΔH_m and their melting points T_m (Sato *et al.*, 1989, Arishima *et al.*, 1991, Rousset and Rappaz, 1996). The melting points, T_m, and the melting enthalpies, ΔH_m, of the polymorphs increase with their stability (Sangwal and Sato, 2012).

The formation of the metastable polymorphs is usually suppressed by increasing the crystallisation temperature (Sangwal and Sato, 2012). Upon formation of the metastable forms, *α* and *β'*, the system tends to favour their transformation into the thermodynamically stable phase, *β*, in order to lower its free energy (Sangwal and Sato, 2012).

It can be said that the crystallisation of fats is a complex occurrence which depends on a variety of factors such as the crystallisation temperature, the crystallisation kinetics of different polymorphs, the presence of impurities and its concentration (Sangwal and Sato, 2012).

2.3. Shear Thinning and Thixotropic Behaviour

The rheology of fat systems is important for its use in the food industry as it may need to be pumped to various locations in a factory. Fat networks exhibit two rheological behaviour named pseudoplasticity and thixotropy. Pseudoplasticity (shear thinning) is a non-Newtonian flow phenomenon in which an increase in shear rate results in a decrease in viscosity (Triantafillopoulos, 1988). Mechanisms responsible for this rheological behaviour include (Triantafillopoulos, 1988):

- Structure-breaking due to hydrodynamic effects where the rate of particle dissociation is greater than that of association
- Favourable orientation of macromolecules or dispersed asymmetric particles in the flow field

Thixotropy is defined as the ability of a system to recover all or part of its structure after deformation through shear. It can also be defined as an isothermal, reversible reduction in viscosity with shear rate. The rheograms of thixotropic fluids are characterised by a hysteresis loop between the increasing shear rate curve (up curve) and the decreasing shear rate curve (down curve), illustrated in Figure 2.5. This area is a measure of the thixotropic breakdown of a system and is assumed to measure power loss during a test cycle. The structure of a thixotropic material reforms upon cessation of flow, and so the amount of thixotropic breakdown is sensitive to shear history, the rate of change of shear, and its maximum value (Triantafillopoulos, 1988).

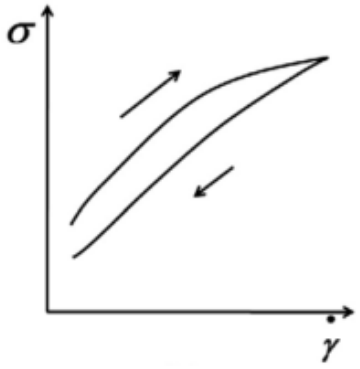

Figure 2.5: Schematic of a typical hysteresis loop (Mewis and Wagner, 2009).

Because "thixotropy reflects the finite time taken to move from one state of microstructure to another and back again", all liquids with microstructure can exhibit thixotropy (Barnes, 1997). Microstructural change in flow occurs as a result of the competition between break-down due to flow stresses, build up due to in-flow collisions and also Brownian motion. In some cases the opposite of thixotropy is observed (antithixotropy, or rheopexy), where flow results in structuring and rest in destructuring of a material (Barnes, 1997). This is when existing weakly attached microstructural elements (resulting from in-flow collisions) are slowly disintegrated as a result of the random actions of Brownian motion (Barnes, 1997).

The time needed for the microstructure of materials to return to their initial state can range from seconds to hours and rebuilding of structure usually takes much longer than breakdown (Barnes, 1997). The true steady-state behaviour of a thixotropic liquid is observed after an infinite shearing time at a given shear rate or stress, or at an infinite rest time. However it is possible to come close to such state after a 'reasonable' time rather than an infinite time because such equilibrium states are approached asymptotically (Barnes, 1997).

2.4. Fractality

In 1982 Benoit Mandelbrot suggested the concept of fractal geometry (Mandelbrot, 1982) as a method of quantifying natural objects with a complex geometrical structure which could not be quantified by regular geometrical methods (Euclidean geometry) (Narine and Marangoni, 1999b). Ideal, man-made, or regular objects are most appropriate for quantification by Euclidean geometry. Objects have integer dimensions in classical Euclidean geometry; for instance a line is a one dimensional object, a plane is two-dimensional and a volume is three-dimensional (Narine and Marangoni, 1999b).

However the object formed from the introduction of enough twists and bends in a line may be classified as being an intermediate between a line and a plane, or a plane and a cube whose dimension would be fractional – *i.e.* between 1 and 2, or between 2 and 3. Such object could be classified as a fractal object as it has a fractional dimension instead of having an Euclidean dimension (Narine and Marangoni, 1999b).

Self-similarity (the repetition of patterns in the object at many different scales) is one of the most important features of fractal objects. For example a tree has branches, these branches have smaller branches and so on, and a very similar pattern is observed at different scales of observation (Narine and Marangoni, 1999b). Euclidean geometry falls short when it comes to quantification of self-similar natural objects such as clouds, coastlines, trees, etc., but fractal geometry can be used to provide quantification for such objects with non-integral dimensions (Narine and Marangoni, 1999b).

Fractal geometry can also be used for quantification of a disordered distribution of mass, such as a cluster of stars in a galaxy or the clustering of particles in a colloid. Equation 2.2

gives the relationship between mass and radius for a solid two-dimensional disk (Narine and Marangoni, 1999b):

$$M(r) \propto R^2 \qquad \text{Equation 2.2}$$

In this example the object is Euclidean as its dimension is an integer, 2. But for a statistically self-similar disordered distribution of mass the relationship between the radius and mass may be given by equation 2.3 (Narine and Marangoni, 1999b):

$$M(r) \propto R^D \qquad \text{Equation 2.3}$$

where *D* is the fractal dimension. It has been experimentally shown that the fractal nature of the microstructure dominates the elastic properties of fat crystal networks at low solid fat contents (Vreeker *et al.*, 1992) and at high solid fat contents (Marangoni and Rousseau, 1996, Marangoni and Rousseau, 1998a, Marangoni and Rousseau, 1998b).

The relationship between the shear elastic modulus (G') and the fractal nature of a fat crystal network is shown in Equation 2.4 (Narine and Marangoni, 1999b).

$$G' \sim \Phi^m \qquad \text{Equation 2.4}$$

where Φ is the particle volume fraction of the solid fat and *m* depends on the fractal dimension of the fat network.

2.5. Quantification of Fat Networks Using Fractal Dimensions

Fat networks are made up of interconnecting fat crystal clusters and because fat crystal clusters are typically irregularly shaped and have a heterogeneous size distribution, it is not easy to quantify their structure or to build a numerical model relating the morphology of the fat crystal clusters to their physical properties (Tang and Marangoni, 2006b). Fractal geometry provides a new concept to understand many natural phenomena (Narine and

Marangoni, 1999b). The fractal nature of fat crystal networks was first recognised by Vreeker *et al.* (1992) and further explored by Tang and Marangoni (2006b). Fractal geometry can be applied to fat crystal networks as they exhibit a certain degree of similarity in structure at different scales of observation, Figure 2.6. Fractal dimensions describe the combined effects of crystal morphology and the spatial distribution patterns of crystal clusters in fat crystal networks (Tang and Marangoni, 2006b).

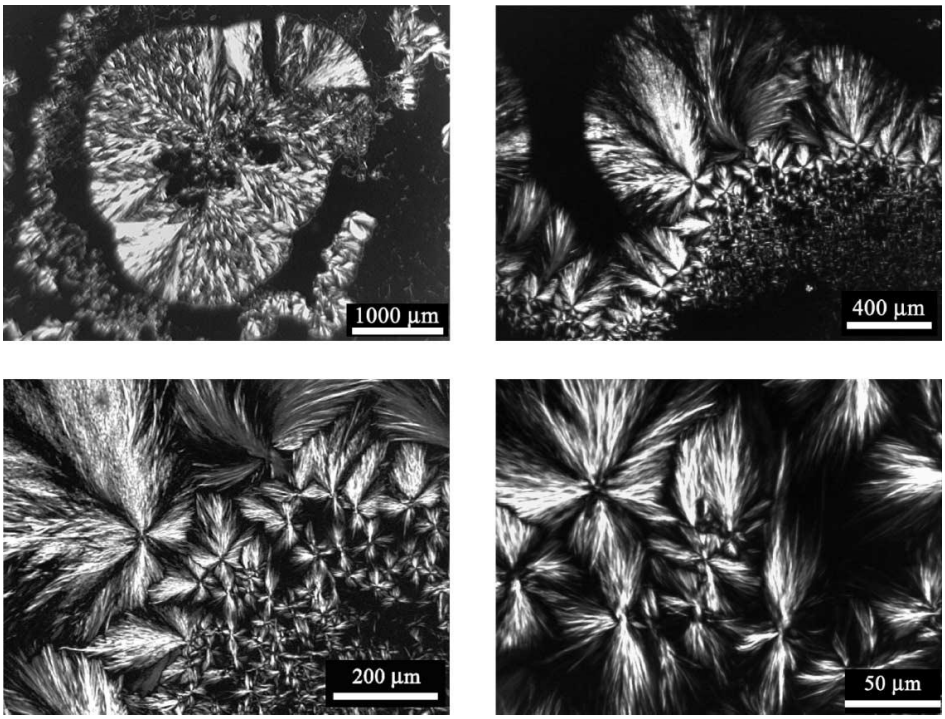

Figure 2.6: Polarised light images of crystalline structures of a fat system at different magnifications (Marangoni, 2002).

2.5.1. Fractal Dimension by Rheological Methods

Because of the similarities between fat crystal networks and colloidal gels, a theory related to the scaling behaviour of the elastic properties of colloidal gels has been adapted for fat crystal networks (Narine and Marangoni, 1999b). This theory, which was submitted by Shih *et al*. (1990), refers to the scaling of the elastic properties of colloidal gels under two

regimes that depend on the strength of the inter-cluster links relative to the strength of the clusters themselves. The model suggests the 'strong-link regime' which is applicable to colloidal gels at low particle concentrations, and the 'weak-link regime' which is applicable at high particle concentrations (Narine and Marangoni, 1999b).

In the strong-link regime the individual clusters grow large and act like a weak spring, and the elastic constant of the system as a function of particle concentration is dominated by the elastic constant of the clusters (Narine and Marangoni, 1999b), and is given by Equation 2.5 (Shih *et al.*, 1990):

$$G' \sim \Phi^{[(d+x)/(d-D)]} \qquad \text{Equation 2.5}$$

where x is the tortuosity of the network, and d is the Euclidean dimension. In the weak-link regime the 'inter-microstructural' links are weaker than the 'intra-microstructural' links and so the elastic constant of the system is governed by the elastic constant of the links between the clusters. Equation 2.6 describes the suggested relationship.

$$G' \sim \Phi^{[(d-2)/(d-D)]} \qquad \text{Equation 2.6}$$

From such theoretical basis, the elastic modulus increases in a power law manner as a function of Φ (Narine and Marangoni, 1999b).

2.5.2. Fractal Dimension by Microscopy Methods

The fractal dimension of a fat system can be calculated by various microscopy methods such as box counting, particle counting, and Fourier transformation using polarised light micro-graphs (Tang and Marangoni, 2006b). The fractal dimension of a system is used to quantify the variation in length, area, volume, or other properties with changes in the scale of the measurement interval (Avnir *et al.*, 1985) and is an intensive property of a fractal object (Tang and Marangoni, 2006a). Due to the fractal nature of fat crystal networks,

fractal dimensions can be used to describe the combined effects of morphology and spatial distribution patterns of the crystal clusters in fat crystal networks (Tang and Marangoni, 2006b).

In order to calculate the microscopy fractal dimension of an object, a property of the fractal object such as its length, is measured at different length scales (Tang and Marangoni, 2006b). The fractal dimension of the object is obtained from the exponential term of the power law relationship between length of the object and the length scale. This principle is used to calculate the box-counting (see next section), particle-counting, and Fourier-transform fractal dimensions. These methods differ in the properties measured and also the formula used to obtain the fractal dimensions from the exponential term (Tang and Marangoni, 2006b).

2.5.2.1. Box-counting Fractal Dimension, D_b

The box-counting method can be used to obtain the box-counting fractal dimension, D_b, of a system. In order to achieve this square grids with side length l_i are placed over the PLM images of fat crystal networks. If a grid contains pixels of the object it is considered as an occupied grid, and the number of the occupied grids, N_i, for the corresponding side length, l_i, is counted; this is repeated for grids with varying side lengths (Tang and Marangoni, 2006c).

Because of the fractal nature of fat crystal networks, a power law relationship exists between the number of occupied grids and the grid's side length, and so the plot of $log(N_i)$ vs $log(l_i)$ is linear (Sikorski and Sikorska-Wisniewska, 2006). The negative gradient of this log-log plot is the box-counting fractal dimension, D_b, of the system (Tang and Marangoni, 2006a), as described by Equation 2.7.

$$D_b = -\frac{\Delta \ln(N_i)}{\Delta \ln(l_i)}$$ Equation 2.7

As previously mentioned, fat crystal networks are complex structures formed through crystallisation of fats, which is in its own right very complicated and is affected by a variety of parameters. Because fat crystal networks greatly influence the properties of the final products they are in, it is important to understand how they are affected by the formulation and processing conditions during production in order to be able to reduce the saturated fat levels while maintaining the physical properties of the fat systems.

3. MATERIALS AND METHODS

3.1. Formulation and Processing

All of the studies carried in this report used commercially available rapeseed oil, obtained from Sainsbury's, UK. The study looking into the effects of solid fat composition on the properties of fat networks (section 4.1) used as its solid fat, hydrogenated palm kernel oil (Sil-Cream 90) obtained from Silbury Marketing Ltd., Warwick, UK. All other studies looking into the effects of A-unit mixing speed, coolant temperature and throughput (sections 4.2, 4.3, and 4.4 respectively) used glyceryl tripalmitate (tripalmitin) obtained from Sigma-Aldrich Company Ltd., Dorset, UK, as the solid fat. All materials were used without further purification.

For the study looking into the effects of solid fat composition on properties of the system mixtures of 5, 10, 20, and 30 w/w% hydrogenated palm kernel oil (Sil-Cream 90) and rapeseed oil were used. The different mixtures were then processed in the A-unit at a constant pump speed (throughput) of 35 ml/min, scraper speed of 1200 rpm, and coolant temperature of 15 °C. All other studies looking into the effects of A-unit mixing speed, coolant temperature, and throughput on the properties of fat systems used mixtures of 5 w/w% tripalmitin and 95 w/w% rapeseed oil were used.

In all studies the fat mixtures were heated to 80 °C and kept at that temperature for 90 minutes in order to erase crystal history of the solid fats. All samples were made in triplicates 2 hours prior to characterisation and upon exiting the A-unit the samples were stored at 20 °C.

In the experiments conducted to study the effects of mixing speed of the A-unit on the fat systems the mixtures were processed at various mixing speeds (400, 800, 1200, and 1500 rpm) at a constant 35 ml/min throughput, and at a constant 5 °C coolant temperature.

For the study looking into the effects of coolant temperature the fat mixtures were processed at different coolant temperatures (2, 5, 10, and 15 °C) at a constant throughput of 35 ml/min, and at a constant A-unit mixing speed of 1200 rpm.

In the study of the effects of throughput on the properties of fat systems the mixtures were processed at various throughput rates (35, 90, 150, 190, and 220 ml/min) at constant mixing speed of 1200 rpm, and at constant coolant temperature of 5 °C.

3.1.1. A-Unit

The production of yellow fat spreads such as margarine or mayonnaise in the food industry takes place in a series of three units A, B, and C (a scraped surface heat exchanger, a cooling tunnel, and a pin stirrer). The scraped surface heat exchanger is the first of the three units and is therefore usually referred to as the A-unit. This unit was used to crystallise the high-melting fats and produce fat crystal networks. The A-unit used in this study has an internal diameter of 3.1 cm; Figures 3.1a, 3.1b and 3.1c show the disassembled unit.

a)

b)

Figure 3.1: Images of the disassembled A-unit showing the shaft, scraper blades and the jacketed unit cover. a) Side view; b) Side view; c) Top view of shaft, and bottom view of the cover.

Figure 3.2 is a schematic of the experimental set-up used for the production of fat systems. The feed to the bench-scale scraped surface heat exchanger is a liquid mixture of high- and low-melting fats at 80 °C. Thermocouples were placed in various positions to measure the temperature of the fats at such points. The large internal surface area of the A-unit available for crystallisation and the mixing of newly formed crystals, scraped from the surface by the scraping blades, into the bulk fat enable rapid crystallisation.

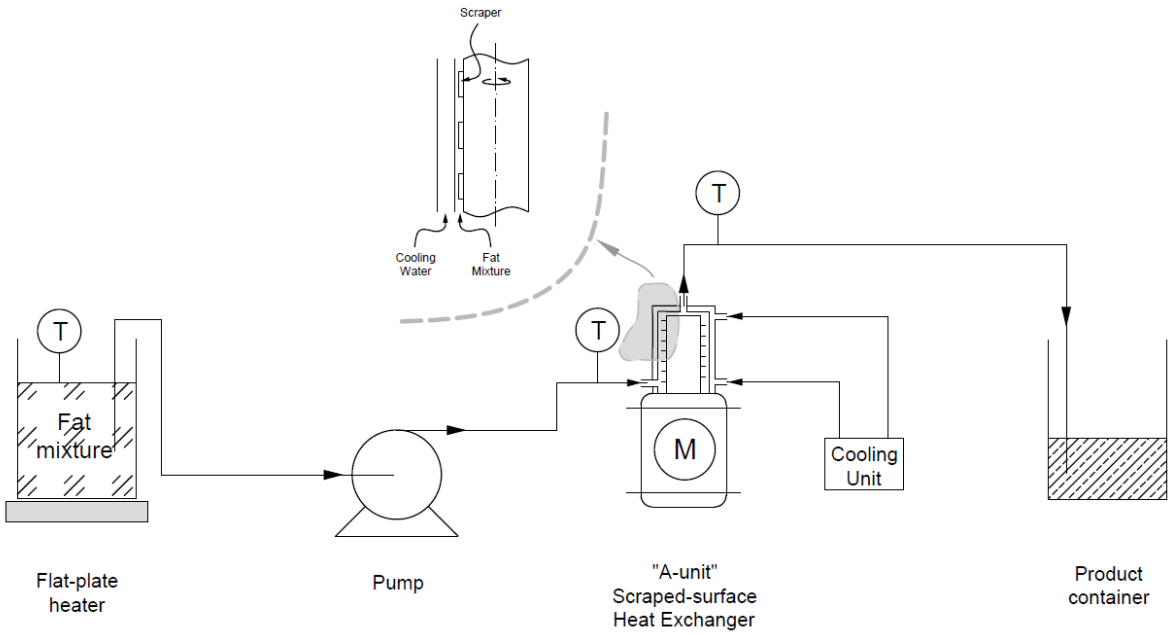

Figure 3.2: Schematic diagram showing the experimental set-up for the production of fat crystal networks using the A-unit. 'T' are thermocouples used for record the temperature; and 'M' is the motor which rotates the scraper shaft inside the A-unit.

The A-unit operates as a continuous unit, with a horizontal inlet at the bottom side and a vertical outlet centred on the top wall aligned with the shaft. The rotating shaft possesses 13 scrapers, which scrape off the crystallised fat from the stationary sides of the unit.

3.2. Rheological Measurements

All of the rheological measurements carried out in this study were done so using a Malvern Instruments Kinexus 500 Rheometer equipped with a roughened-surface parallel plate geometry with a gap size of 1 mm between the upper and lower plates. All experiments were done in triplicates and the temperature of the sample in between the two plates was controlled using a Peltier element allowing the samples to be analysed at 20 °C for all experiments apart from those studying the effect of temperature on viscosity.

3.2.1. Viscometry

The effect of shear rate on the viscosity of the samples was studied. For this a shear rate table was used to increase the shear rate from 0.01 s^{-1} to 100 s^{-1} (ramp-up) and then to return from 100 s^{-1} to 0.01 s^{-1} (ramp-down) for the study of the effect of solid fat composition on fat systems. In all other studies the samples were tested at a wider range of shear rates, 0.01 s^{-1} to 1000 s^{-1} for the ramp-up and 1000 s^{-1} to 0.01 s^{-1} for the ramp-down.

The effect of temperature on the fat systems was studied using a temperature loop (20 °C to 30 °C to 20 °C at a rate of 2 °C/min) at a constant shear rate of 0.05 s^{-1}.

3.2.2. Oscillatory Rheology

Rheological measurements at small deformations were performed for all of the studies. Amplitude sweeps were carried out to determine the Linear Viscoelastic Region (LVR) of the systems so they could then be studied for their elastic (G') and viscous (G'') moduli. The LVR is where the stress increases with strain at a constant rate (Tang and Marangoni, 2006b) and is below the point at which the dynamic properties change drastically with increasing strain (Phan-Thien and Safari-Ardi, 1998). Strain controlled oscillatory amplitude sweeps from 0.01 to 10%, at a constant frequency of 1 Hz were carried out for each sample to obtain its LVR. Frequency sweeps were subsequently carried out to obtain the G' and G'' values using the strain value identified to be within the LVR. The frequency ranges were 0.1-10 Hz for the study of the effects of solid fat composition, and 0.1-100 Hz for all other studies.

3.2.3. Thixotropy

During the thixotropic loop experiments the samples were subjected to two consecutive loops of increasing and decreasing shear rates at 20 °C. The samples were subjected to an

increasing rate ramp (0.01 – 100 s^{-1}), held at 100 s^{-1} for 2 minutes, and were then subjected to a decreasing rate ramp (100 – 0.01 s^{-1}), which concluded the first thixotropic loop and after which the loop was repeated once more on the same sample.

3.3. Polarised Light Microscopy (PLM)

Polarised light microscopy was used to visualise the microstructure of the fat crystal networks. In order to achieve this a small droplet of the fat system exiting the A-unit was placed on a microscope slide. A cover slip was then placed parallel to the plane of the slide and centred on the drop of sample to ensure uniform sample thickness. The microscope slides and cover were purchased from Fisher Scientific, Loughborough, UK. Images were taken using a Canon 1000D DSLR camera mounted on an SP300F polarised light microscope obtained from Brunel Microscopes Ltd., Chippenham, UK. A minimum of six images were taken of each sample.

3.3.1. Image Processing and Fractal Dimension Determination

PLM images were processed using the image processing software ImageJ, National Institutes of Health, USA. The original PLM images were initially converted to 8-bit greyscale. They were then thresholded manually to a satisfactory level at which the actual microstructure of the fat systems, as observed under polarised light, were all represented; Figure 3.3 shows an example of this process, which is similar to the method used in the literature (Awad *et al.*, 2004).

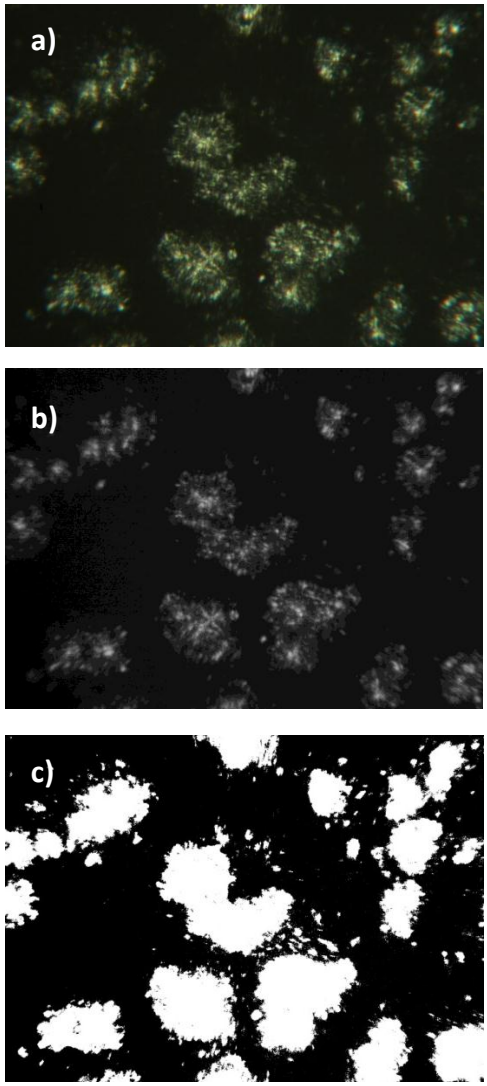

Figure 3.3: The step-by-step transformation of a typical PLM image; a) Original image; b) Converted 8-bit Greyscale image; and c) The thresholded image.

Following the processing steps required for the analysis the PLM images were used to obtain the box-counting fractal dimensions (D_b) of different fat systems. The D_b of the processed images were obtained following analysis using 'FracLac 2.5', which is a freely available plug-in for ImageJ developed by Audrey Karperien, Charles Sturt University, Australia.

3.4. Differential Scanning Calorimetry (DSC)

Differential scanning calorimetry (DSC) was used to study the melting and crystallisation behaviour of various fat systems. In preparation for the experiments samples of a known weight (8-15 mg) were transferred into aluminium pans, which were then hermetically sealed; an empty aluminium pan was used as a reference pan.

For the study of the effects of solid fat composition a Diamond DSC, obtained from Perkin Elmer, UK was used to obtain the crystallisation and melting profiles of the fat systems. This study investigated the effects of formulation on the melting and crystallisation behaviours of fat systems. For these experiments the samples were inserted into the equipment at 20 °C and held at that temperature for 10 minutes, following which they were heated to 60 °C at a rate of 10 °C/min. The samples were held at 60 °C for 10 minutes before being cooled to -20 °C at a cooling rate of 10 °C/min, and held at this temperature for 10 minutes. The samples were then heated from -20 °C to 60 °C at a rate of 10 °C/min.

All other studies investigated the effects of processing conditions on the melting behaviour of fat systems and used a heating program in which the samples were inserted at 20 °C and held at such temperature for 5 minutes, after which they were heated to 80 °C at a rate of 10 °C/min. The equipment used for these studies was a Perkin Elmer DSC7 obtained from Perkin Elmer, UK. The results of these experiments are shown in the Appendix.

4. RESULTS

4.1. Effects of Solid Fat Composition

This section focuses on how the physical properties of the fat systems are affected by its solid fat composition. Figure 4.1 illustrates how the viscosity of fat system is affected by the solid fat composition of the system.

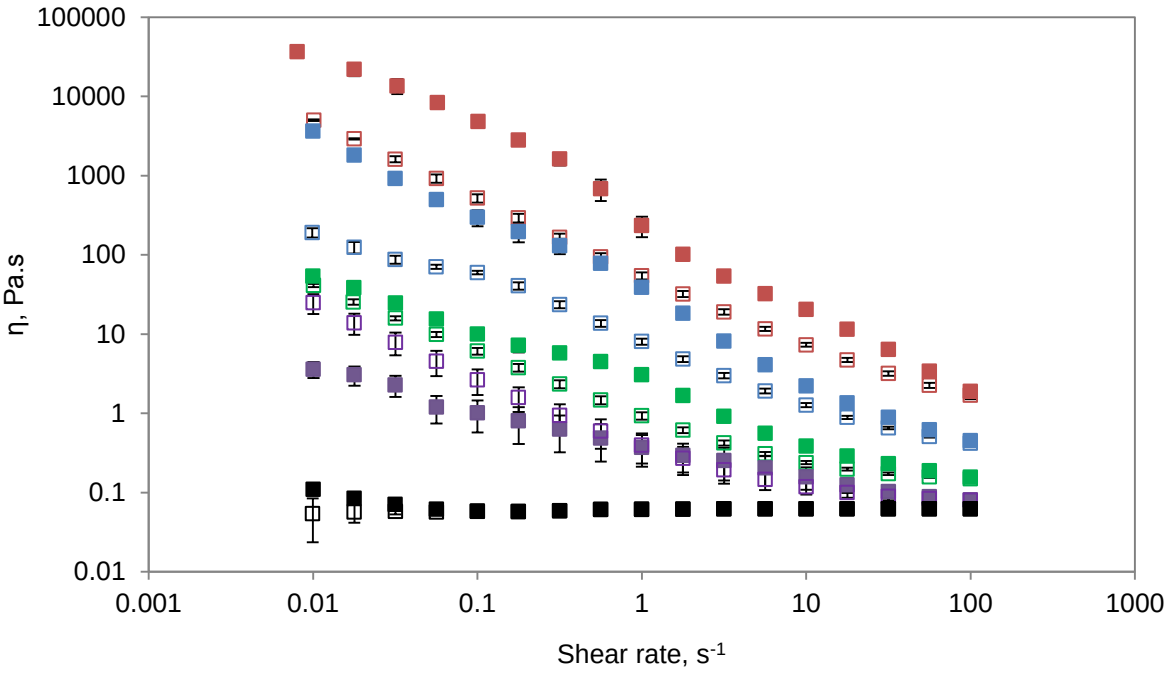

Figure 4.1: Plot of viscosity against shear rate for samples with different concentrations of solid fat. (▪) Fat system containing 30% solid fat, shear ramp-up; (▫) 30% solid fat, shear ramp-down; (▪) 20% solid fat, shear ramp-up; (▫) 20% solid fat, shear ramp-down; (▪) 10% solid fat, shear ramp-up; (▫) 10% solid fat, shear ramp-down; (▪) 5% solid fat, shear ramp-up; (▫) 5% solid fat, shear ramp-down; (▪) Rapeseed oil only, shear ramp-up; (▫) Rapeseed oil only, shear ramp-down.

Study of the effect of shear rate on the viscosity of the systems produced at various solid fat compositions showed that the fat systems were shear thinning, see Figure 4.1. This is because as the shear rate increases the links between the crystal clusters are broken resulting in a decrease in viscosity. This is in contrast to the Newtonian behaviour of rapeseed oil, whose viscosity profile is constant with varying shear rate.

It is also observed that at the end of the experiment the viscosities of samples containing high levels of solid fats (*i.e.* 20% and 30%), at the same shear rate (0.01 s^{-1}), are lower than those at the start of the experiment. This reflects on the thixotropic behaviour of fat systems and indicates that the links between the crystal clusters, which are broken through the course of the experiment, have not been reformed during the timeframe of the experiment. The opposite is observed for the sample containing low levels of solid fats (*i.e.* 5%). Rheopectic behaviour (the opposite of thixotropic behaviour) is exhibited by the 5% solid fat sample. This means that the application of shear has altered the microstructure of the sample's fat system in such a way that results in an increase in viscosity.

Samples containing 10% solid fat behaved in an intermediate manner between the two previously mentioned behaviours. The viscosities of such samples did not seem to change either way (at 0.01 s^{-1}). Figure 4.1 also shows that increasing the amount of solid fat in the system increases its viscosity by a considerable amount across all shear rates. This is because increasing the solid fat composition means a higher proportion of the system is available to crystallise, which in turn results in the formation of a stronger network and hence an increase in the viscosity of the system. This is further illustrated in Figure 4.2.

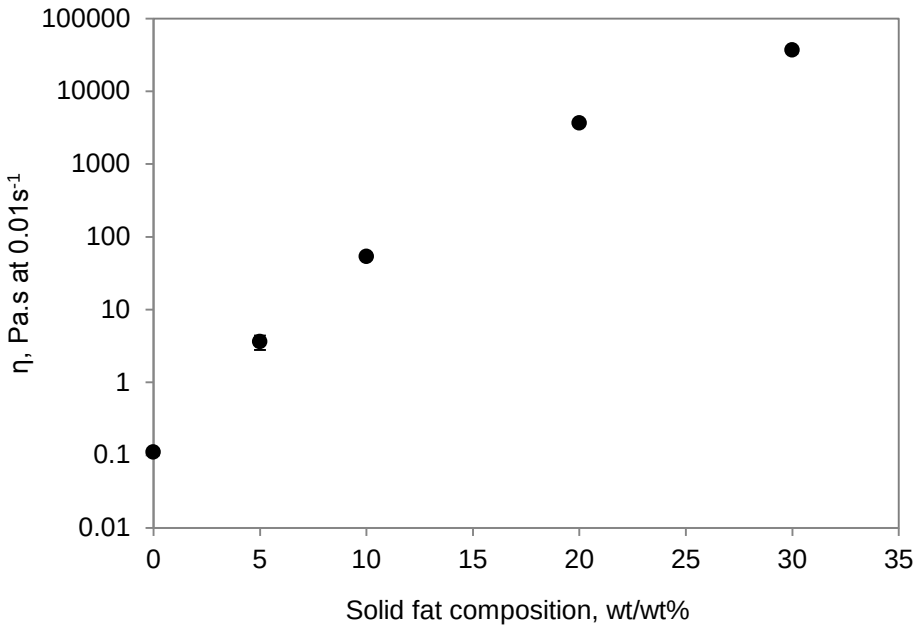

Figure 4.2: Plot of viscosity versus solid fat composition at shear rate of 0.01 s^{-1}.

Figure 4.2 shows that increasing the solid fat composition of the system (0, 5, 10, 20, and 30%) results in an exponential increase in the viscosity of the system. This is because a stronger network, containing more crystalline clusters, is formed.

Figure 4.3 shows how temperature affects the viscosity of fat systems. A typical sample was subjected to a constant shear rate and the temperature of the set-up increased from 20 °C to 30 °C at a rate of 2 °C/min; followed by a decrease in temperature from 30 °C to 20 °C at the same rate.

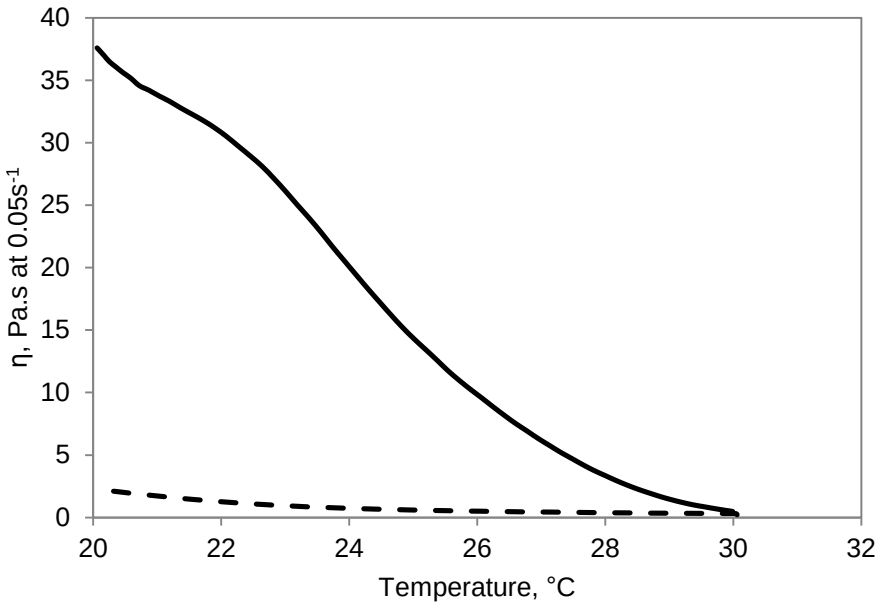

Figure 4.3: Plot illustrating the effect of temperature on viscosity for a sample containing 10% hydrogenated palm kernel oil (solid fat) at a heating and cooling rate of 2 °C/min and at a constant shear rate of 0.05 s^{-1}. Solid line (—) represents the temperature ramp-up; Dotted line (---) represents the temperature ramp-down.

It can be seen from Figure 4.3 that the viscosity decreases rapidly as the temperature is raised to 30 °C. This is because the fat crystal clusters in the network melt as the temperature increases. This goes hand in hand with the observations made by Marangoni and McGauley (2002) when investigating the effect of temperature on the D_b of cocoa butter, where they observed a reduction in the complexity of structure (indicated by a decrease in D_b) with increasing temperature. It should also be pointed out that the viscosity of the system does not build back up to the initial value as the temperature is returned to 20 °C. This is because the high-saturates proportion of the system has not had enough time to form crystals under test conditions; so at this point, there are little or no crystals present in the fat system.

Amplitude sweeps were carried out on all of the samples in order to determine their Linear Viscoelastic Region (LVR), which was then used to conduct frequency sweep tests to study the elastic and viscous moduli of the systems. Figure 4.4 is a graphical illustration of the results for a typical amplitude sweep test; from which the LVR can clearly be identified.

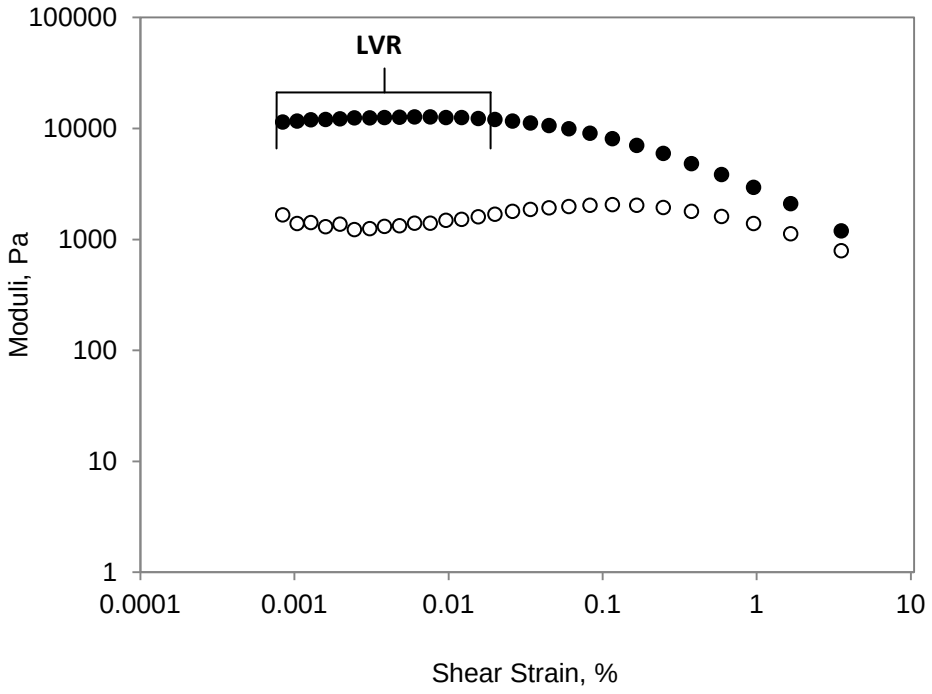

Figure 4.4: Amplitude sweep plot of sample containing 20% solid fat, showing the LVR. (●) Represents G'; (○) Represents G''.

Figure 4.5 is a plot of viscous (G'') and elastic (G') moduli versus frequency for samples with different solid fat compositions.

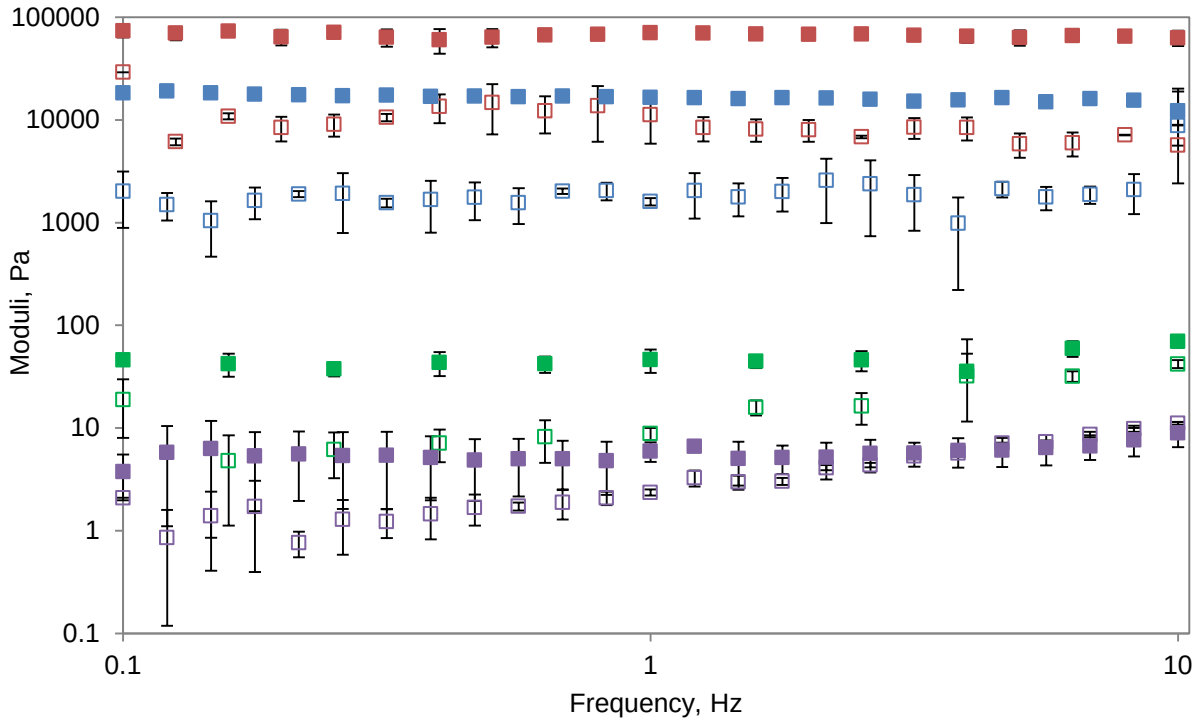

Figure 4.5: Plot of G' and G'' versus Frequency. (▪) Represents G' of samples containing 30% solid fat; (▫) Represents G'' of samples containing 30% solid fat; (▪) Represents G' of samples containing 20% solid fat; (▫) Represents G'' of samples containing 20% solid fat; (▪) Represents G' of samples containing 10% solid fat; (▫) Represents G'' of samples containing 10% solid fat; (▪) Represents G' of samples containing 5% solid fat; (▫) Represents G'' of samples containing 5% solid fat.

The fat systems tested are shown to be solid-like as their G' values are higher than their G'' values, Figure 4.5. It should be mentioned that this is not the case for the system containing 5% solid fat. Cross-over of the elastic and viscous moduli is observed for this system; *i.e.* at various frequencies the system containing 5% solid fat has a higher G'' value compared to its G', and is therefore more liquid-like. Figure 4.5 also shows that increasing the amount of solid fat in the system results in an increase of the values of the system's elastic and viscous moduli. This is complementary to the results of the viscometry experiments.

The following, Figure 4.6, shows the relationship between the elastic and viscous moduli, and the solid fat composition of the fat system.

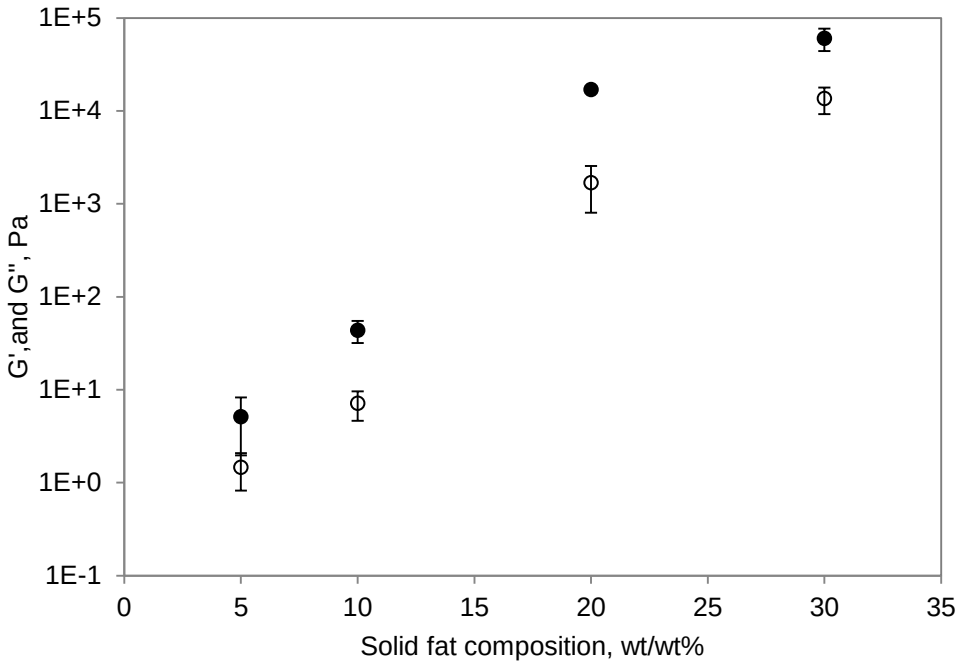

Figure 4.6: Plot of elastic modulus and viscous moduli (at 0.1 Hz) against the solid fat composition of the systems. (●) Represents G'; (○) Represents G''.

Figure 4.6 above, illustrates how the elastic and viscous moduli changes as a result of increasing the amount of solid fat in the system at low frequencies (0.4 Hz in this case); a non-linear increase is observed for both G' and G''. This is similar to a study carried out by Higaki *et al.* (2004) in which they observed an increase in both the elastic and the viscous moduli of fat systems, containing śāl (Shorea robusta) fat olein and fully hydrogenated rapeseed oil with high amounts of behenic acid, with increasing solid fat.

Polarised Light Microscopy was used to observe the microstructure of the system, and to visualise the fat crystal network. Figure 4.7 illustrates how varying the concentration of solid fat alters the microstructure of the fat system as observed through PLM.

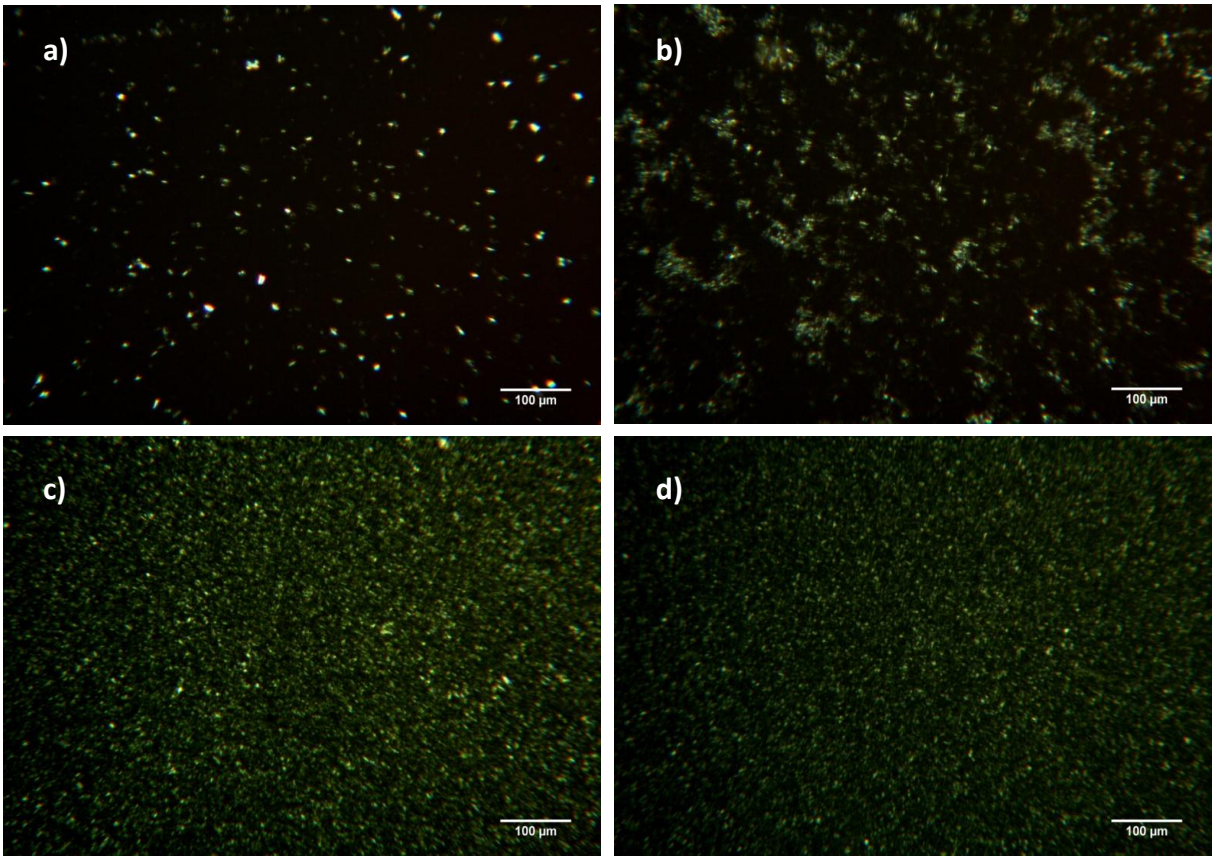

Figure 4.7: PLM images of the microstructure of fat networks a) 5 wt/wt% solid fat; b) 10 wt/wt% solid fat; c) 20 wt/wt% solid fat; d) 30 wt/wt% solid fat.

Figure 4.7 visually indicates that the amount of crystals present increases with increasing solids composition. This is similar to the study carried out by Awad *et al.* (2004) in which they took PLM images of fat systems containing different amounts of solid fat in order to study the scaling behaviour of the elastic modulus in such fat systems. This explains the increase in the viscosity and the moduli of samples containing higher amounts of solid fat. This is because the presence of higher amounts of solid fat results in the formation of a higher amount of fat crystals which in turn results in more interactions and thus a stronger fat crystal network.

Figure 4.8 shows the various types of crystals which can be formed with time.

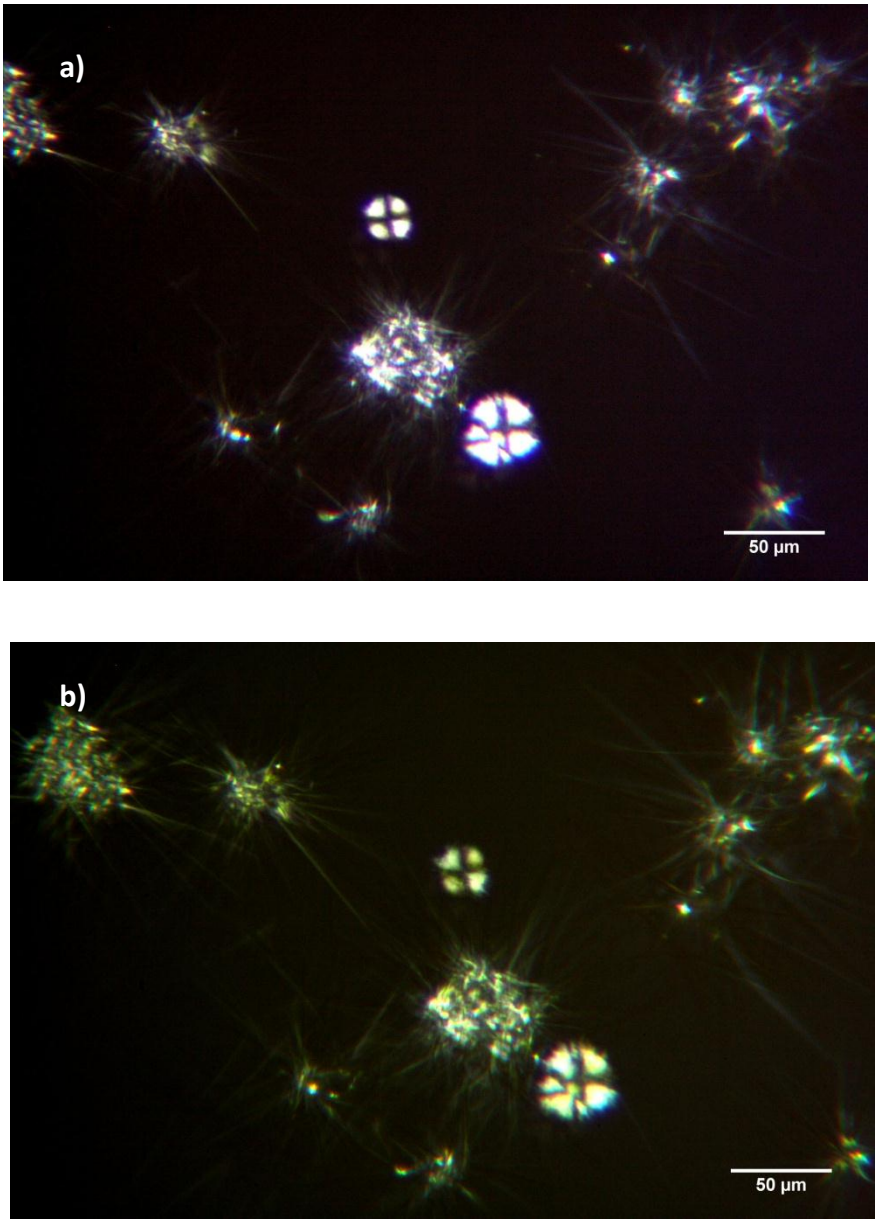

Figure 4.8: PLM images of a sample containing 20 wt/wt% solid fat. a) Taken on day 3 after production; b) Taken on the 9th day after production.

Figure 4.8 shows the formation and growth of certain types of crystals. The presence of needle-like crystal, spherulitic clusters (with their rough surface visible), and the more smooth spherulitic crystals (which appear to have a Maltese cross through them) is observed. The growth of some of these crystals is also observed in Figure 4.8; as it can be seen there are fewer needle-like crystals visible in the image taken on day 3 after

production, and they are shorter in length in comparison to the image of the same area taken 9 days after production.

In addition for use to visualise the microstructure of the fat systems, polarised light microscopy (PLM) was also used in order to quantify the microstructure of the system by calculating the fractal dimension of the network. Figure 4.9 shows how the fractal dimension of the fat systems, D_b, changes with increasing solid fat composition.

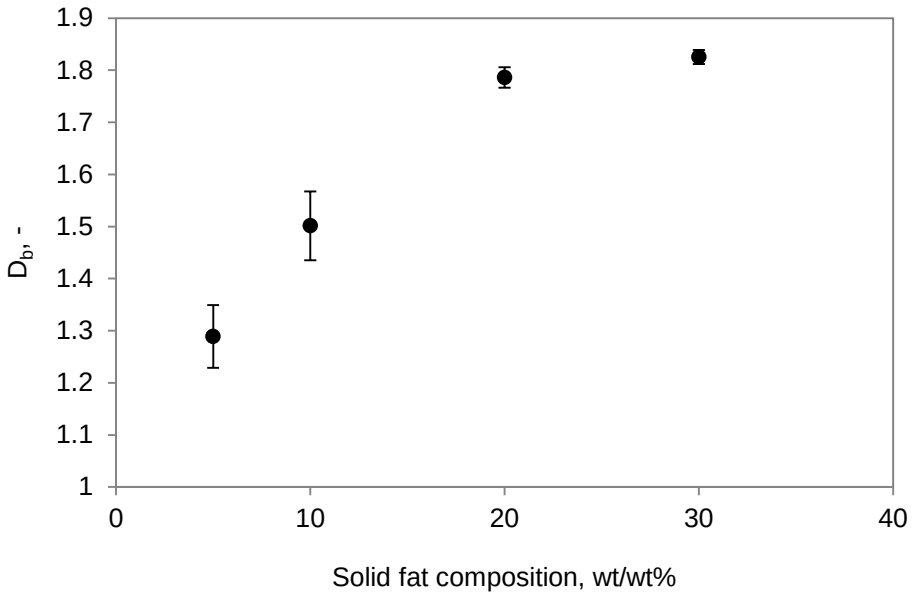

Figure 4.9: Changes in the box counting fractal dimension (D_b) as a function of solid fat composition of the samples.

Figure 4.9 shows that increasing the solid fat composition of the system results in an increase in its fractal dimension calculated by *FracLac 2.5* which uses Equation 2.7. This is because more crystals are formed as a result of the presence of higher amounts of solid fats in the system. This in turn leads to higher levels of complexity which is portrayed in the fractal dimension of the system. This correlates with the literature on the effects of complexity on the fractal dimension; Corbit and Garbary (1995) investigated the shape

complexity of the fronds of three species of brown algae during plant development and found that fractal dimension increased with increasing complexity of shape. Figure 4.9 shows that the fractal dimensions plateau with increasing solid fat; this is because of the geometric restrictions of the two-dimensional space in which the microstructure of the fat network was observed, *i.e.* the fractal dimensions obtained are 2-D fractal dimensions, as they were acquired using 2-D PLM images, and so cannot have a value of greater than 2.

It should be mentioned that the method of acquiring the fractal dimension of fat systems through PLM images (used in this study) is not an accurate method as it is subject to human errors during the manual thresholding step, as simply thresholding the images at a different value can have significant effects on the value of D_b obtained. Furthermore the alternative methods of automatic thresholding, or thresholding at a single value for images are not feasible, due to the fact that each image is different and represents a specific section of the microstructure, and different images also contains different levels of light. The visual differences in the microstructure are minimised for samples containing similar amounts of solid fats and therefore the effect of human error becomes more prominent. For this reason further studies will cease to use fractal analysis as a method of characterisation of the fat systems.

The effect of varying the solid fat composition of fat systems on their melting and crystallising behaviour was observed using differential scanning calorimetry. Below are the heating, Figure 4.10a, and cooling, Figure 4.10b, profiles of fat systems containing different amounts of solid fat.

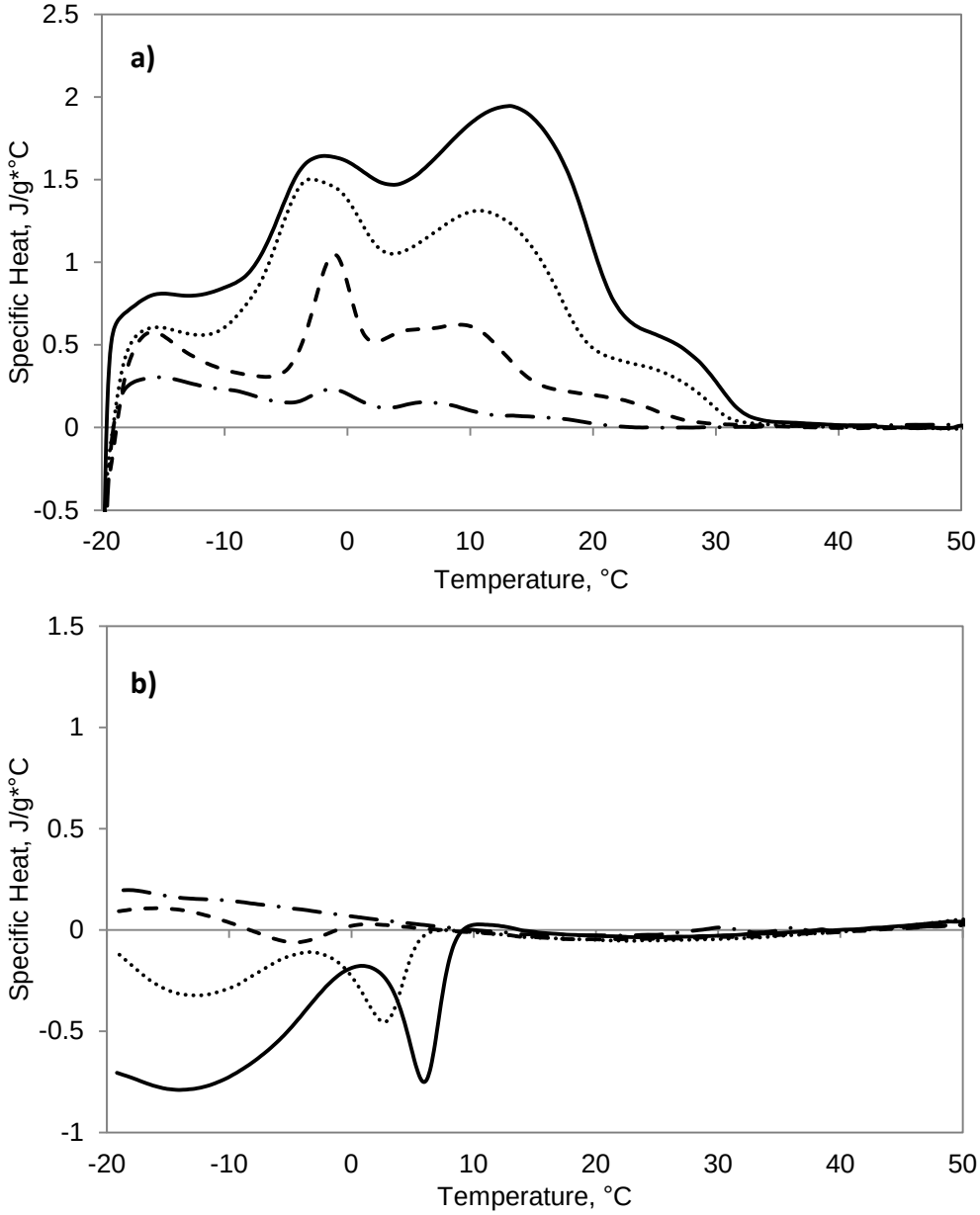

Figure 4.10a) DSC profiles of the melting behaviour; b) DSC profiles of the crystallisation behaviour of samples containing varying amounts of solid fats. (—) Represents samples containing 30% solid fat; (···) Represents samples containing 20% solid fat; (– –) represents samples containing 10% solid fat; (— · —) Represents samples containing 5% solid fat.

It can be seen from Figure 4.10a that increasing the solid fat composition results in an increase in the amount of energy required to melt the system and also shifts the maximum melting temperature to higher values; this is because of numerous interactions occurring

between different TAGs, giving rise to the formation of crystals containing various amounts of the low- and high-melting components, and the presence of an increased number of high-melting crystals. This is similar to the results obtained by Shi *et al.* (2005) in a study investigating the effects of adding high- and low-melting fats on the melting profiles of model fat systems. It is observed in Figure 4.10b that the energy released due to crystallisation is larger and that the onset of crystallisation occurs at higher temperatures as the composition of solid fat is increased. Again the reason for this is the presence of increased amounts of high-melting fats, which also crystallise at higher temperatures.

Figure 4.11 shows the relationship between the enthalpy of melting profiles (which is the area under a melting profile) of the systems and their solid fat compositions.

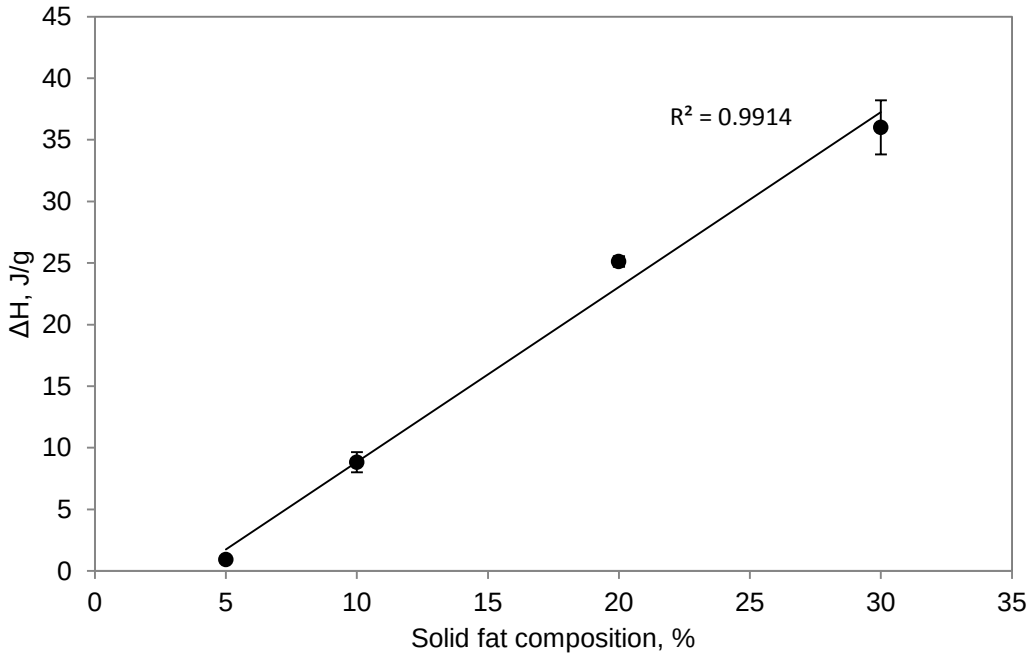

Figure 4.11: Plot of enthalpy (J/g) of melting profiles against the solid fat composition (%) of fat systems.

It is observed from Figure 4.11 that the value of enthalpy increases in a linear fashion with increasing solid fat composition. Thus indicating the reason behind the increase in enthalpy is the presence of higher proportions of solid fat in the fat crystal networks.

4.2. Effects of Mixing Speed

The effect of A-unit mixing speed was studied by producing samples (containing 95% rapeseed oil, and 5% tripalmitin) at different speeds (1500 rpm, 1200 rpm, 800 rpm and 400 rpm), and at a coolant temperature of 5 °C. Figure 4.12 below shows the effect of scraper speed on the viscosity of samples.

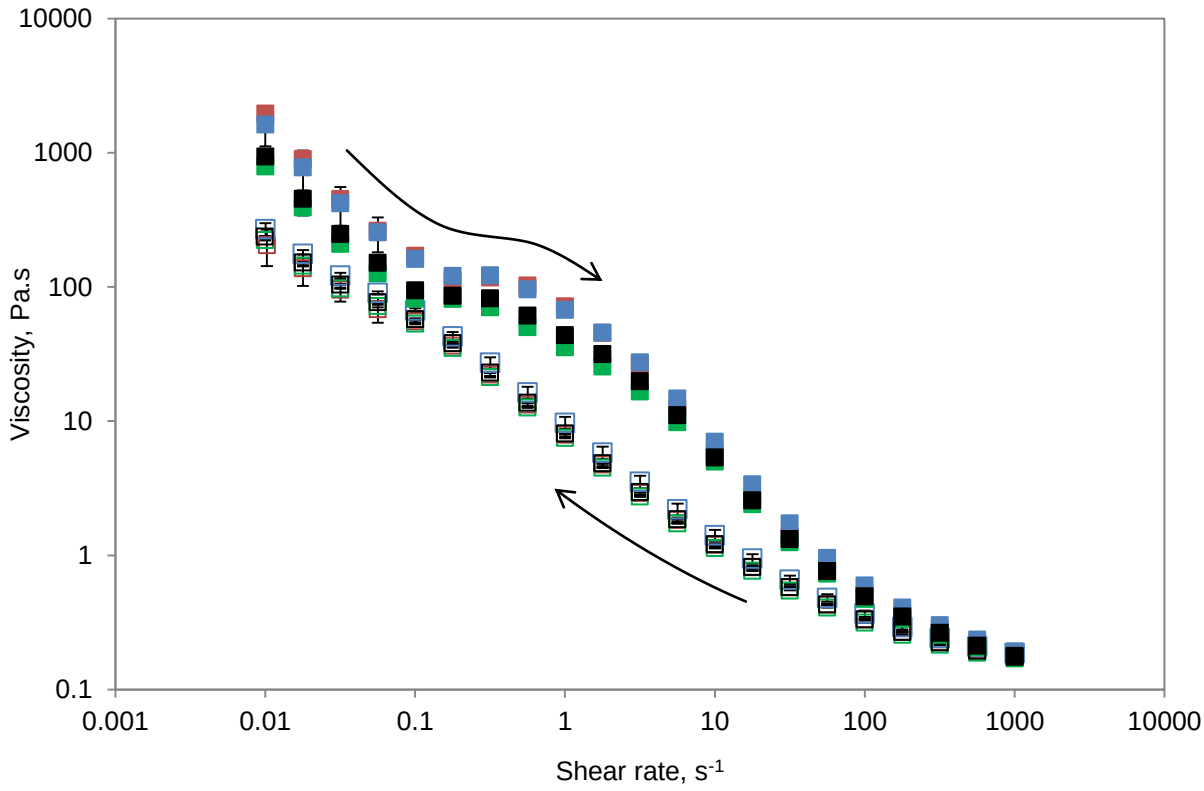

Figure 4.12: Plot of viscosity against shear rate for fat systems produced at different mixing speeds. (■) Represents fat systems produced at 1500 rpm, shear ramp-up; (▫) 1500 rpm, shear ramp-down; (■) 1200 rpm, shear ramp-up; (▫) 1200 rpm, shear ramp-down; (■) 800 rpm, shear ramp-up; (▫) 800 rpm, shear ramp-down; (■) 400 rpm, shear ramp-up; (▫) 400 rpm, shear ramp-down.

All samples in Figure 4.12 show shear thinning and thixotropic behaviour. Microstructural deformation is observed as the viscosity of the system at the end of the experiment is lower than that at the start (both are at the same shear rate, 0.01 s^{-1}). No considerable difference in the viscosity profile is observed between samples produced at various A-unit mixing speeds.

The effect of mixing speed on the elastic and viscous moduli is illustrated in Figure 4.13.

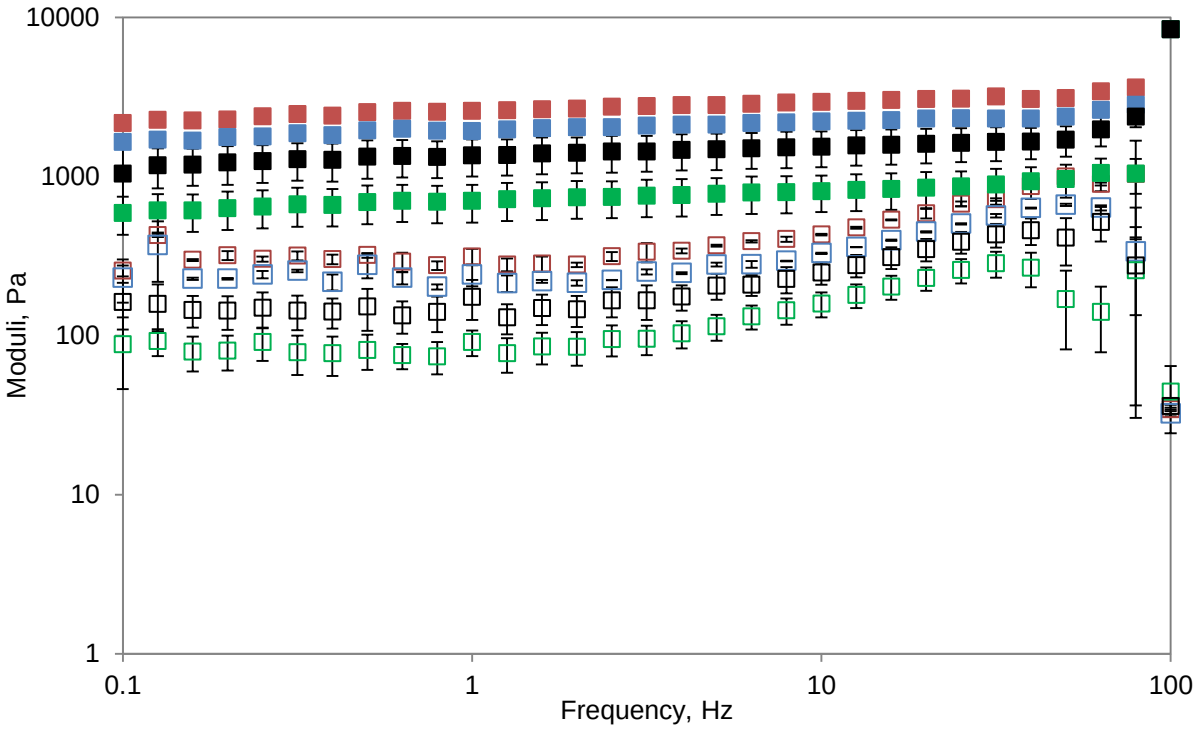

Figure 4.13: Plot of elastic and viscous moduli against frequency for fat systems produced at various mixing speeds. (■) Represents G' of samples made at 1500 rpm; (▫) Represents G'' of samples made at 1500 rpm; (■) Represents G' of samples made at 1200 rpm; (▫) Represents G'' of samples made at 1200 rpm; (■) Represents G' of samples made at 800 rpm; (▫) Represents G'' of samples made at 800 rpm; (■) Represents G' of samples made at 400 rpm; (▫) Represents G'' of samples made at 400 rpm.

The viscous and elastic moduli of samples were found to be very slightly altered by varying the scraper speed. Increasing the mixing speed of the A-unit resulted in a small increase in both the elastic and viscous moduli of the fat systems. A slight increase in value of the elastic and viscous moduli was also observed with increasing frequency. The values of the

viscous moduli however increased significantly with increasing frequency after the 5 Hz mark. At very high frequencies however more erratic behaviour was observed. The fat systems are also shown to behave in a solid-like manner, as their elastic modulus values are greater than that of their viscous modulus.

Fat crystal networks are thixotropic, meaning they undergo structural deformation as a result of shearing, but can recover their initial structure under quiescent conditions if given enough time. Figure 4.14 illustrates the ability of the systems produced at different mixing speeds to recover their original structure following shear deformation. The value of recovery is here defined as the percentage difference between two hysteresis loops carried out on the same sample with no resting time in between the two loops. This is because the hysteresis loop areas refer to the thixotropy of the fat system (Hadnađev *et al.*, 2011).

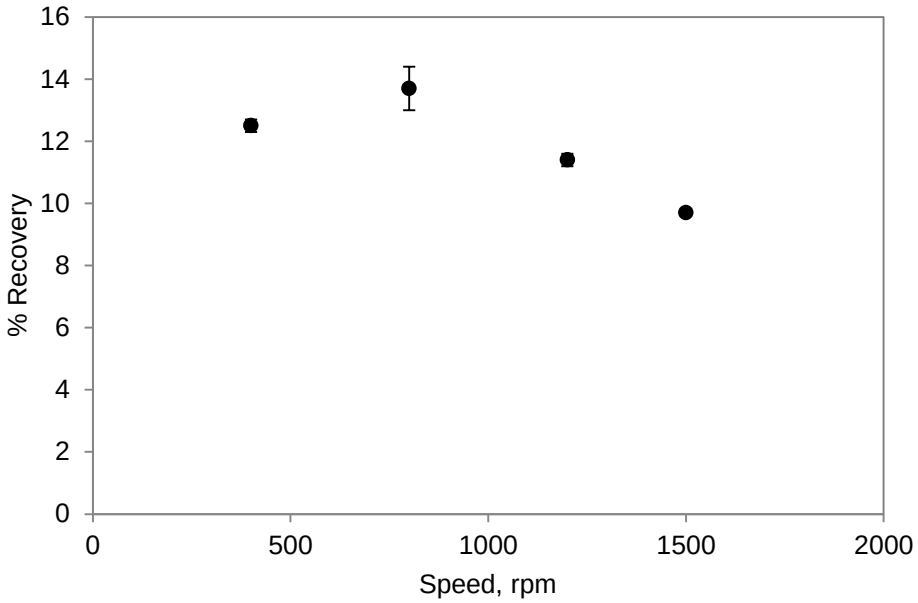

Figure 4.14: Plot of % recovery as a function of A-unit's mixing speed (rpm).

Figure 4.14 shows that the fat systems only recover about 11% of their initial structure during the test; however no significant difference is observed in the recovering ability of fat

systems produced at different mixing speeds. Therefore the A-unit mixing speed does not alter the thixotropic behaviour of fat systems studied.

The melting profiles of the fat systems were studied using differential scanning calorimetry. Figure 4.15 illustrates the effect of mixing speed on the melting peak of the fat systems, which is the temperature at which the specific heat of the system is at a maximum.

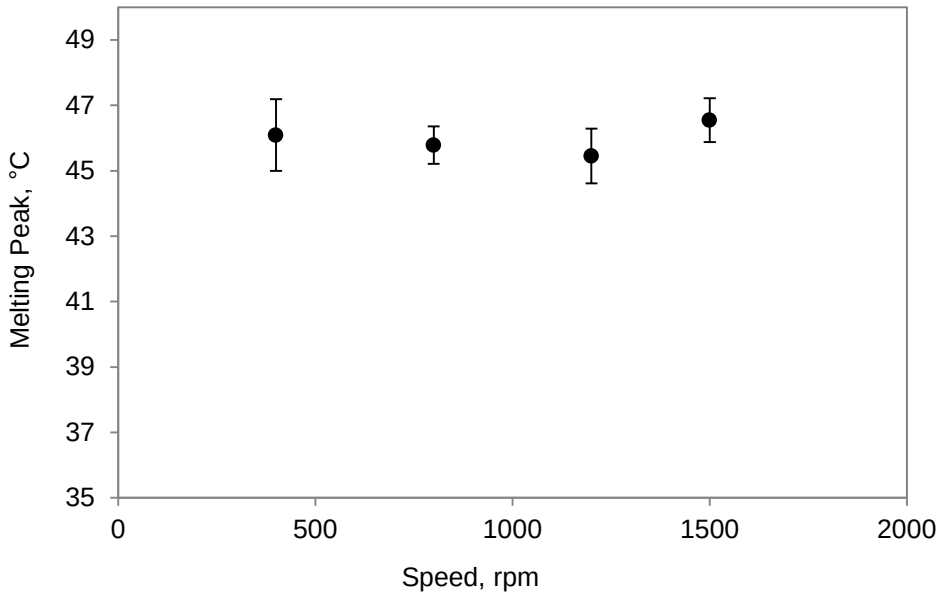

Figure 4.15: Graph of Melting peak (°C) against A-unit's mixing Speed (rpm).

It is observed from Figure 4.15 that the values of the melting peaks of samples produced at various mixing speeds does not change, *i.e.* remains at approximately 46 °C. This indicates that the samples contain the same major polymorphic form of fat crystals. Therefore it can be said that altering the A-unit mixing speed does not alter the type of polymorph formed. Figure 4.16 shows the effect of mixing speed on the enthalpy of fusion of fat systems.

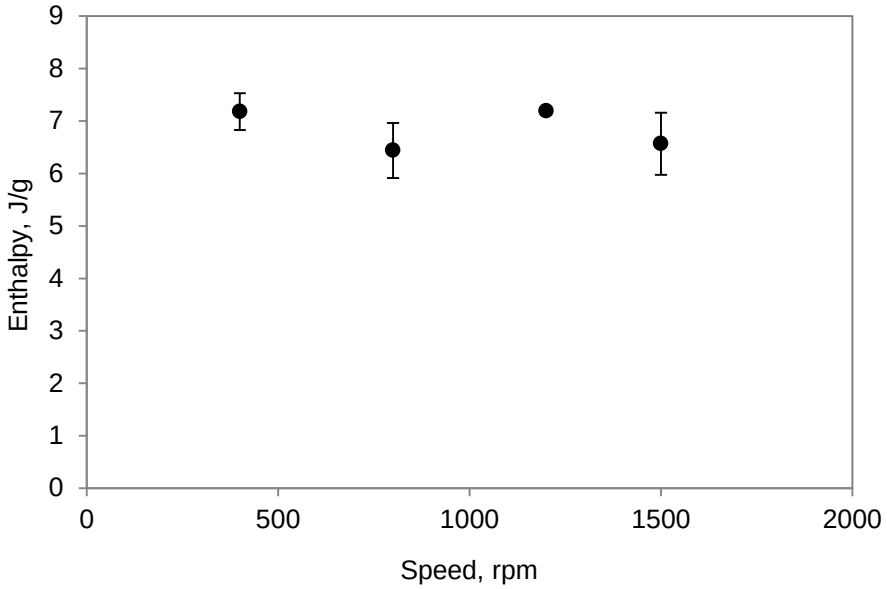

Figure 4.16: Plot of Enthalpy (J/g) of melting profiles against the A-unit mixing speed (rpm).

No significant difference in the values of enthalpy (*i.e.* approximately 7 J/g) is observed for samples produced at different mixing speeds. This indicates that all of the samples contain the same amount of fat crystals, as the energies required to melt the solid fats are equal for all systems.

4.3. Effects of Coolant Temperature

The effect of coolant temperature on the properties of fat systems was studied by producing samples at four different cooling bath temperatures; 15 °C, 10 °C, 5 °C and 2 °C. The effect of the coolant temperature on the viscosity of the fat system is shown in Figure 4.17.

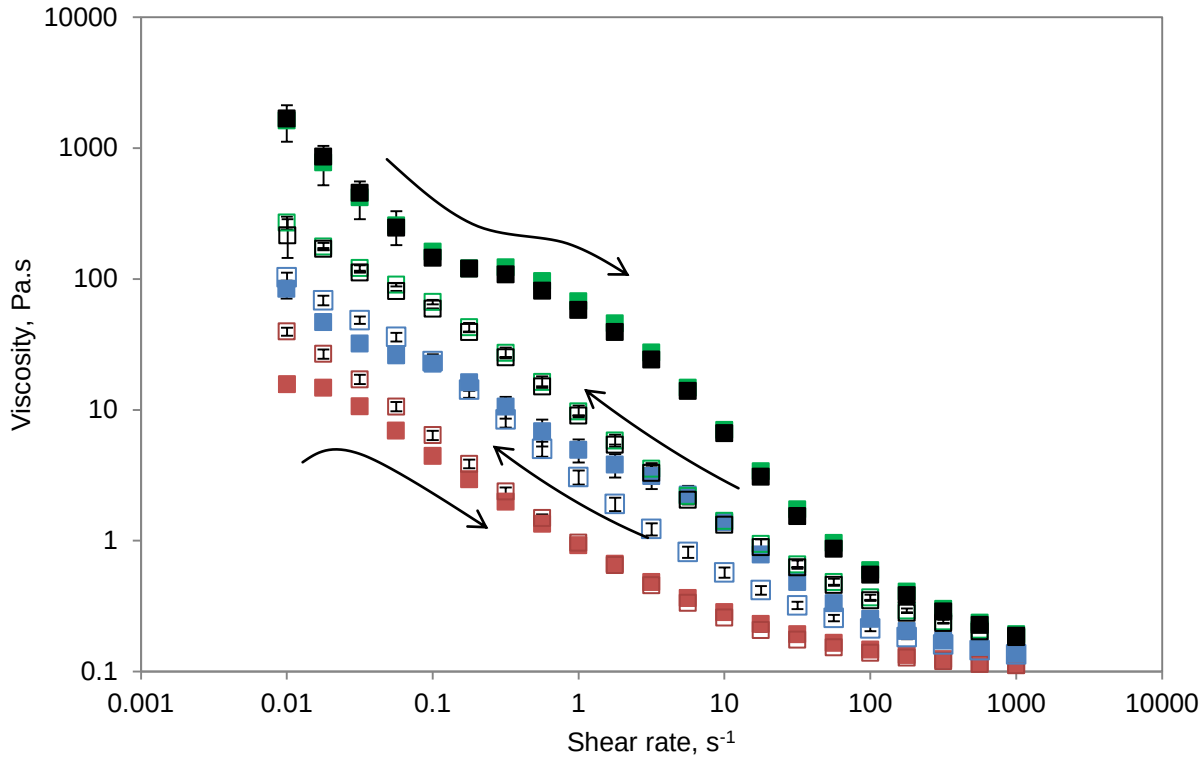

Figure 4.17: Plot of viscosity as a function of shear rate for fat systems produced at different cooling bath temperatures. (■) Represents fat systems produced at 15 °C, shear ramp-up; (□) 15 °C, shear ramp-down; (■) 10 °C, shear ramp-up; (□) 10 °C, shear ramp-down; (■) 5 °C, shear ramp-up; (□) 5 °C, shear ramp-down; (■) 2 °C, shear ramp-up; (□) 2 °C, shear ramp-down.

Figure 4.17 illustrates a general shear thinning behaviour for all of the samples studied. Three different types of viscosity profiles are evident in Figure 4.17. The first, samples produced at low temperatures (*i.e.* 2 °C and 5 °C), show shear thinning behaviour and signs of structural deformation, as they end the experiment with a lower viscosity value compared to the value which they had at the start of the experiment (at the same shear rate). This means that such systems are thixotropic as the links between the crystal clusters, which are broken through the course of the experiment, have not been reformed. This is similar to the observed behaviour of the samples in section 4.2. Figure 4.18 shows the rheological behaviour of this type of viscosity profile.

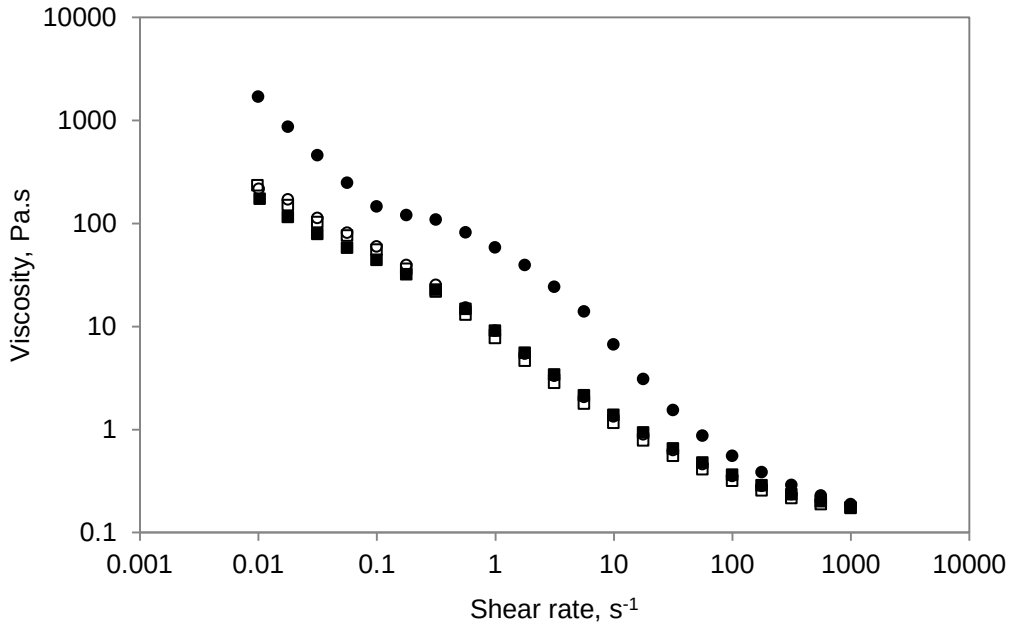

Figure 4.18: Two cycle viscosity profiles of a typical thixotropic sample (produced at a coolant temperature of 2 °C, mixing speed of 1200 rpm and throughput of 35 ml/min). (●) 1st cycle of shear, shear ramp-up; (○) 1st cycle of shear, shear ramp-down; (■) 2nd cycle of shear, shear ramp-up; (▫) 2nd cycle of shear, shear ramp-down.

In Figure 4.18 signs of thixotropic behaviour are observed during the application of the initial cycle of shear rate, this is where the results of the ramp-up and ramp-down of the shear rate are different. However, no further structural deformation is observed by repeat of the application of the shear rate cycle, which immediately follows the initial cycle. In this case the viscosity values at different shear rates, for both the up and down ramps, are the same, indicating the structure does not build back up after the first cycle of shear and thus only shear thinning is observed.

The second type of viscosity profile is that of samples made at a high temperature (*i.e.* 15 °C). Such samples initially exhibit a significant decrease in the viscosity, indicating the shear-thinning nature of solid fat networks with increasing shear rate; and have a higher viscosity at the end of the viscometry experiment, compared to that at the start of the

experiment (at the same shear rate). For these samples the application of shear has altered the microstructure of the systems in such a way that results in an increase in viscosity. Figure 4.19 illustrates the rheological behaviour of this type of system.

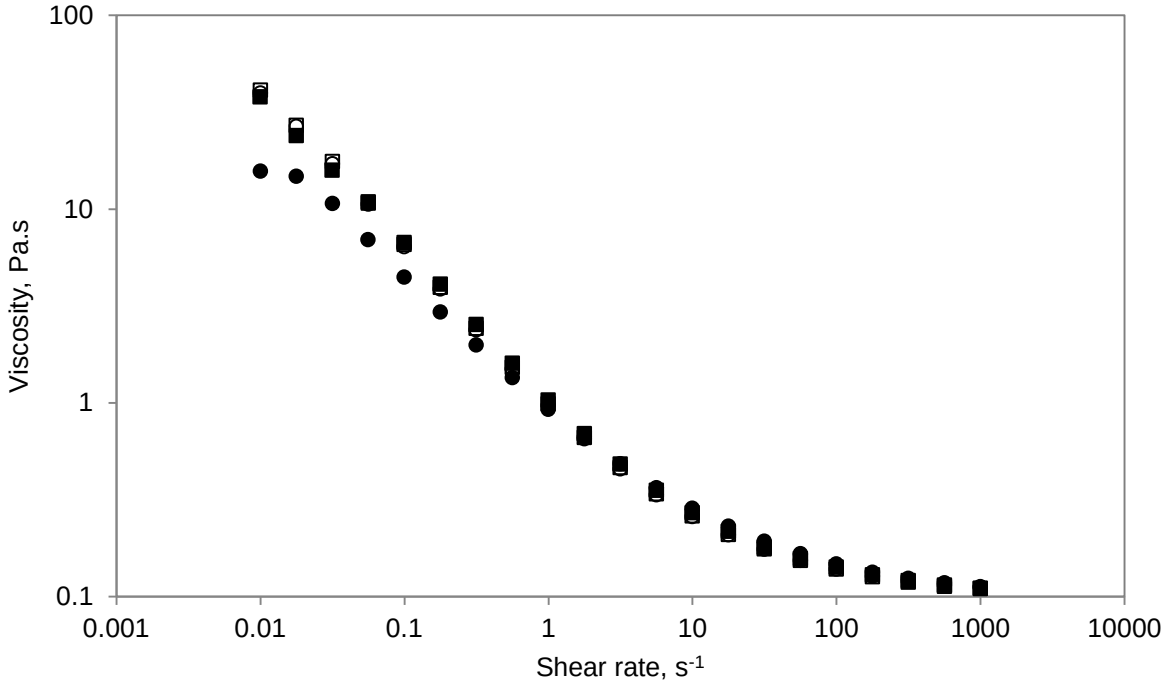

Figure 4.19: Two cycle viscosity profiles of a typical rheopectic sample (produced at a coolant temperature of 15 °C, mixing speed of 1200 rpm and throughput of 35 ml/min). (●) 1st cycle of shear, shear ramp-up; (○) 1st cycle of shear, shear ramp-down; (■) 2nd cycle of shear, shear ramp-up; (□) 2nd cycle of shear, shear ramp-down.

Figure 4.19 shows signs of rheopectic behaviour during the application of the first shear rate cycle. The viscosity of the system is observed to be higher at the end of the experiment (during the ramp-down of shear rate) as compared to the start of the experiment (the ramp-up of shear rate). This increase in the viscosity is, however, only observed during the first cycle as repeating the experiment on the same sample, immediately after the end of the first cycle, does not lead to an increase in the final viscosity value at a specific shear rate.

The third viscosity profile observed in Figure 4.17 is that of samples produced at 10 °C, which behave in a manner intermediate to the two viscosity profiles previously mentioned. At lower shear rates this type of system behaves in a similar way to samples produced at higher temperatures; as a slight increase in viscosity is observed when comparing the values at the start and the end of the experiment. On the other hand the viscosity profile at higher shear rates is similar to that of samples produced at lower temperatures.

The reason for such differences between samples produced at different coolant temperatures is that increasing the coolant temperature reduces the crystallisation ability of the A-unit. This is because lower amounts of energy can be removed from the fat system inside the A-unit as the temperature difference between the coolant and the hot fat system is reduced; therefore the systems exit the unit at a higher temperature, Figure 4.20. As a result of this the amount of type of crystals formed are varied and so giving rise to the difference in the behaviour of systems produced at different coolant temperatures.

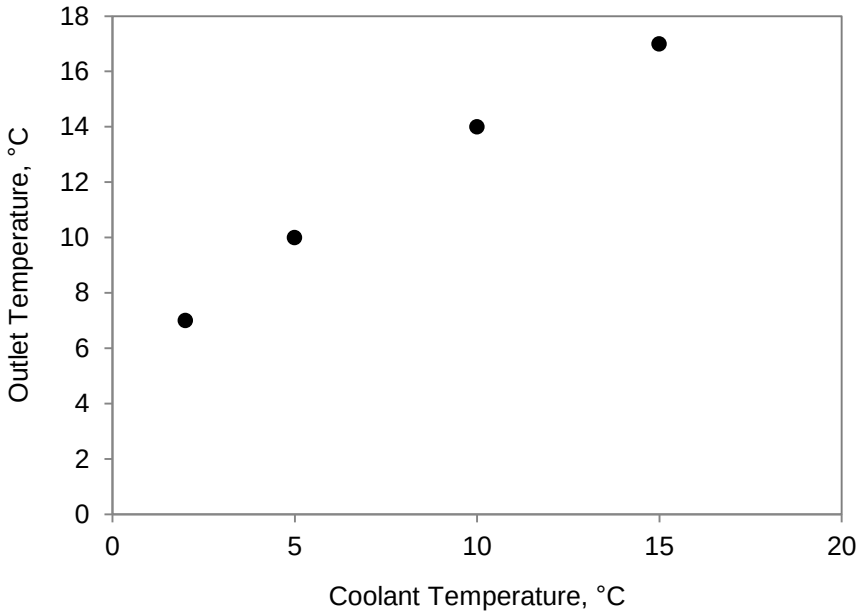

Figure 4.20: Plot showing the effect of coolant temperature on the temperature of the fat system at the outlet of the A-unit.

Figure 4.21 shows the effect of coolant temperature on the viscous and elastic moduli of fat systems.

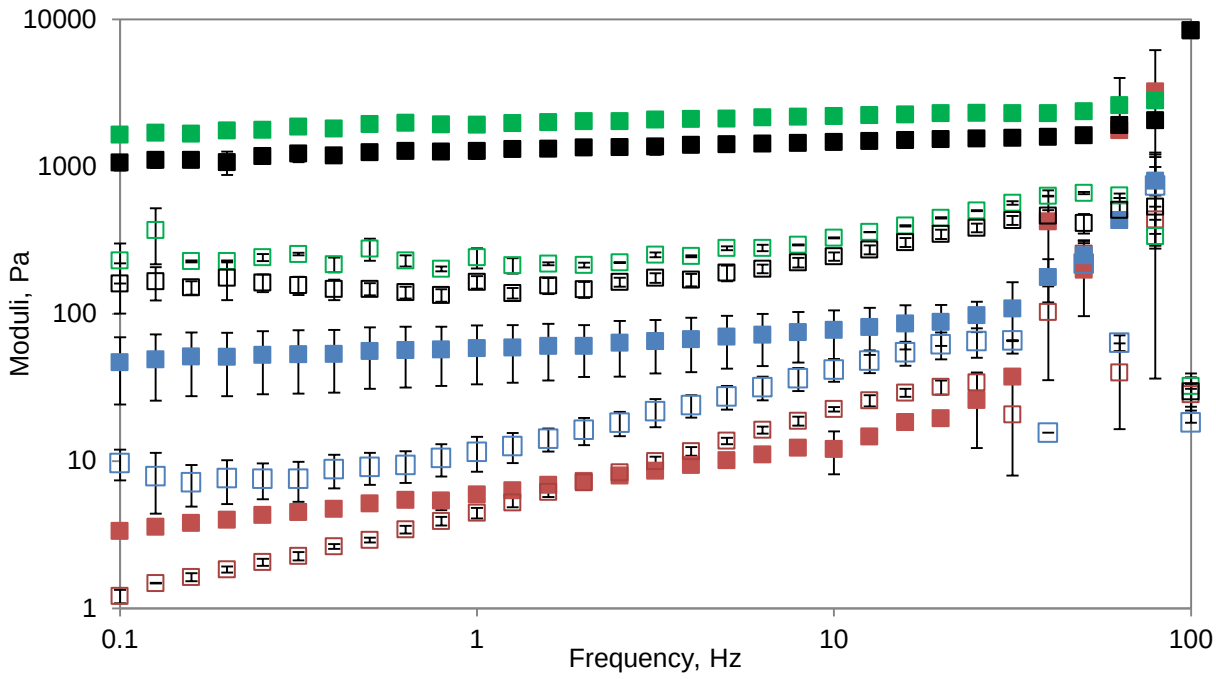

Figure 4.21: Plot of G' and G" against frequency for samples produced at different cooling bath temperatures. (■) Represents G' of samples made at 15 °C; (□) Represents G'' of samples made at 15 °C; (■) Represents G' of samples made at 10 °C; (□) Represents G'' of samples made at 10 °C; (■) Represents G' of samples made at 5 °C; (□) Represents G'' of samples made at 5 °C; (■) Represents G' of samples made at 2 °C; (□) Represents G'' of samples made at 2 °C.

Figure 4.21 shows a general increase in value of viscous and elastic moduli of the fat systems with increasing frequency. For samples produced at higher temperatures (*i.e.* 10 °C and 15 °C), cross-over of moduli was observed, meaning that these samples behave in both solid-like and liquid-like manners depending on the frequency. These samples had a 'cloudy' appearance and were 'quite runny', which indicates the presence of some crystals; but not enough to produce a strong fat crystal network. In contrast the samples produced at lower coolant temperatures were solid-like across the frequency range. The values of the viscous moduli for all of the samples increased significantly and became more irregular at

higher frequencies. The general trend saw moduli values increase with decreasing coolant temperature; however for samples produced at 2 °C and 5 °C this did not hold true, in fact the opposite was observed. However the difference between the moduli of samples produced at 2 °C and 5 °C was relatively small when compared to the difference between the moduli of samples produced at 5 °C and 10 °C for instance. Figure 4.22 shows the ability of fat systems produced at various coolant temperatures to recover their structure after deformation through shear.

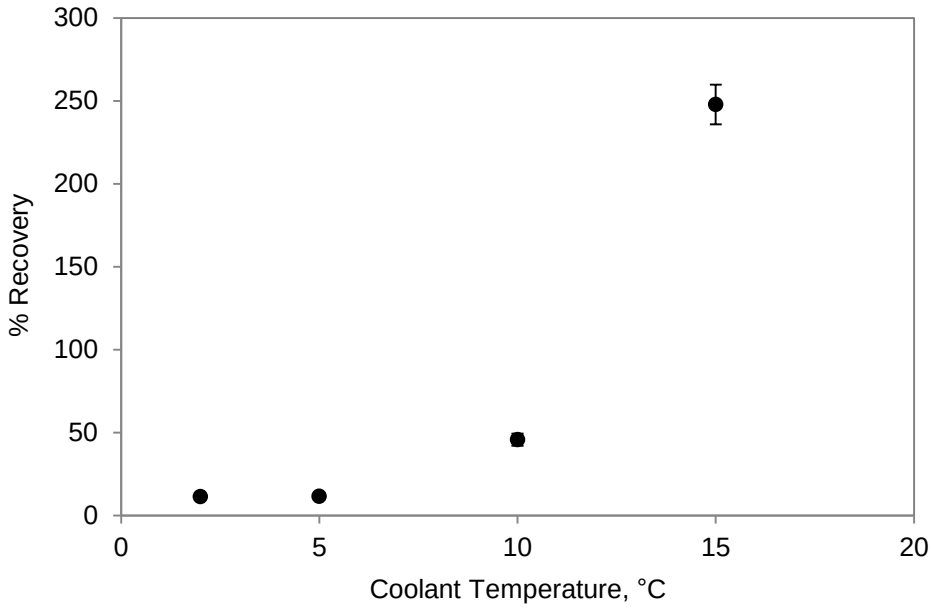

Figure 4.22: Plot of % recovery of the fat systems as a function of coolant temperature.

Figure 4.22 shows that increasing the coolant temperature during production results in the formation of less thixotropic systems. This is illustrated through an increase in the ability of the systems to recover their structure following deformation through shearing. In some cases (for samples produced at a coolant temperature of 15 °C) a recovery of greater than 100% is observed indicating formation (rather than deformation) of structure as a result of shear. This rheopectic behaviour was previously observed and discussed in section 4.1.

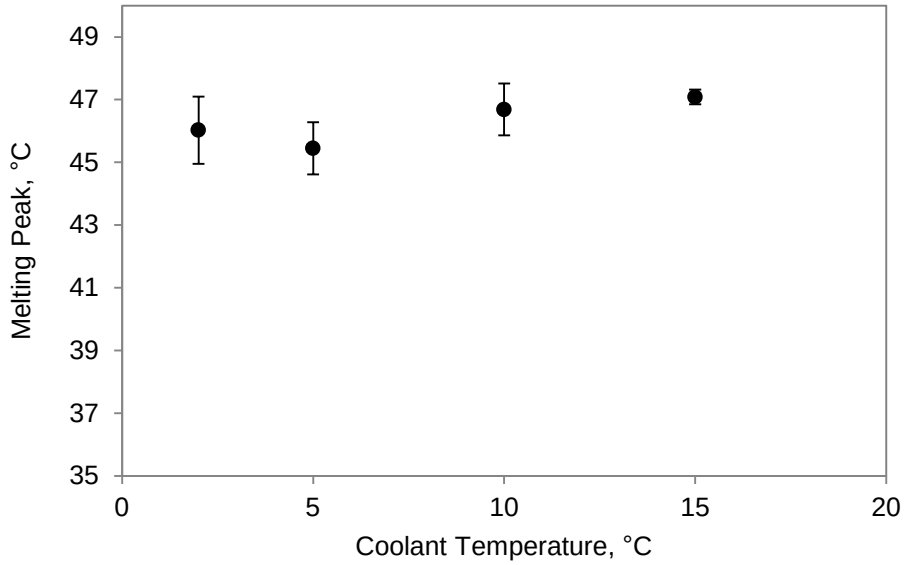

Figure 4.23: Graph of Melting peak (°C) against the A-unit's coolant temperature (°C).

Figure 4.23 shows how the temperature at which the peak of the melting profile occurs, is affected by the temperature of the coolant during the production of the fat systems. It is seen from Figure 4.23 that varying the coolant temperature also does not alter the temperature at which the peak of the melting profile occurs (which stays at approximately 46 °C); indicating that all samples contain the same major polymorphic form. Therefore varying the coolant temperature does not alter the major polymorphic form present in the fat system.

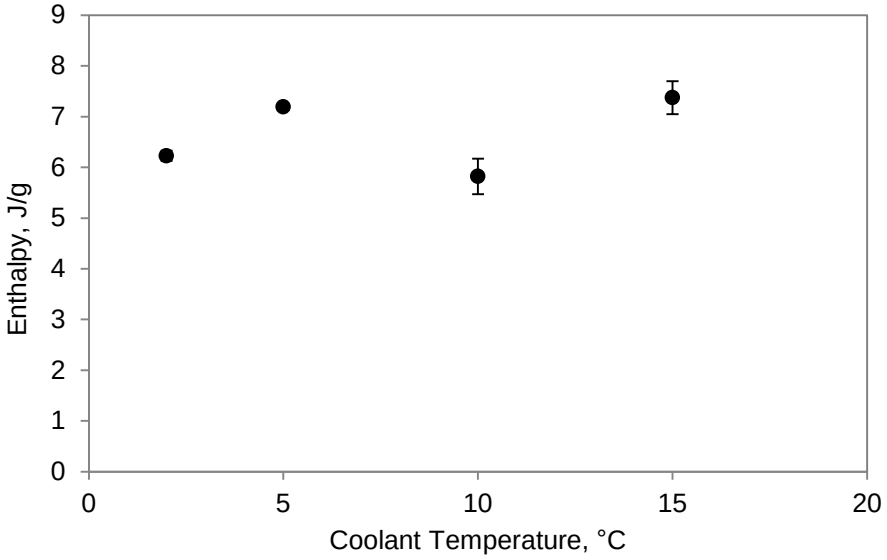

Figure 4.24: Plot of Enthalpy (J/g) of melting profiles against the A-unit coolant temperature (°C).

Figure 4.24 shows how the enthalpy of fusion of fat systems is affected by altering the coolant temperature during production. Again the enthalpy is approximately 7 J/g so there is no significant difference in the enthalpy of fusion of samples produced at various cooling temperatures. This means that the energy required to melt the solids is the same for all of the samples; indicating the samples contain the same amount of solid fat.

4.4. Effects of Throughput

This section looks at the effect of throughput of the A-unit on the properties of fat systems. Samples produced at various throughputs, 35 ml/min, 90 ml/min, 150 ml/min, 190 ml/min, and 220 ml/min were studied. The following, Figure 4.25, shows how the viscosity of the fat system is affected by the throughput.

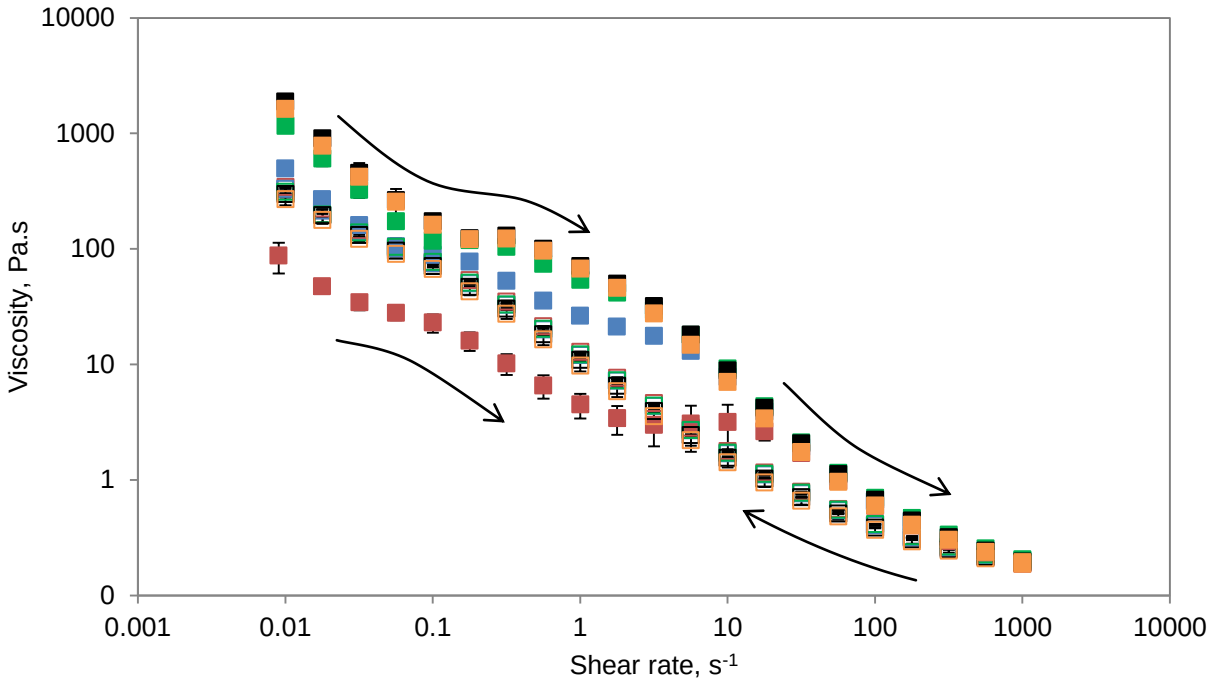

Figure 4.25: Plot of viscosity against shear rate for fat systems produced at different throughputs. (■) Represents samples produced at 220 ml/min, shear ramp-up; (□) 220 ml/min, shear ramp-down; (■) 190 ml/min, shear ramp-up; (□) 190 ml/min, shear ramp-down; (■) 150 ml/min, shear ramp-up; (□) 150 ml/min, shear ramp-down; (■) 90 ml/min, shear ramp-up; (□) 90 ml/min, shear ramp-down; (■) 35 ml/min, shear ramp-up; (□) 35 ml/min, shear ramp-down.

It can be seen that throughput affects the viscosity of the system in a similar way to the coolant temperature, section 4.3, *i.e.* increasing the throughput of the A-unit results in a decrease in the viscosity of the fat systems produced. This is to be expected as increasing the throughput results in shorter residence times in the A-unit, which means the samples spend less time subjected to circumstances within the unit, such as low temperatures, which aid crystallisation; and so as a result of increasing throughput, the fat systems exit the production unit at higher temperatures, Figure 4.26. Another general trend observed from Figure 4.25 is the shear thinning behaviour of the fat systems. Similar to the results from the study into the effects of coolant temperature, altering the throughput of the system results in the production of three distinct types viscosity profiles.

The first type of viscosity profile observed in Figure 4.25 is that of samples produced at low throughput values (35 ml/min, 90 ml/min, and 150 ml/min). Similar to fat systems produced at low coolant temperatures, these systems show shear thinning and thixotropic behaviour (see section 4.3, Figure 4.18).

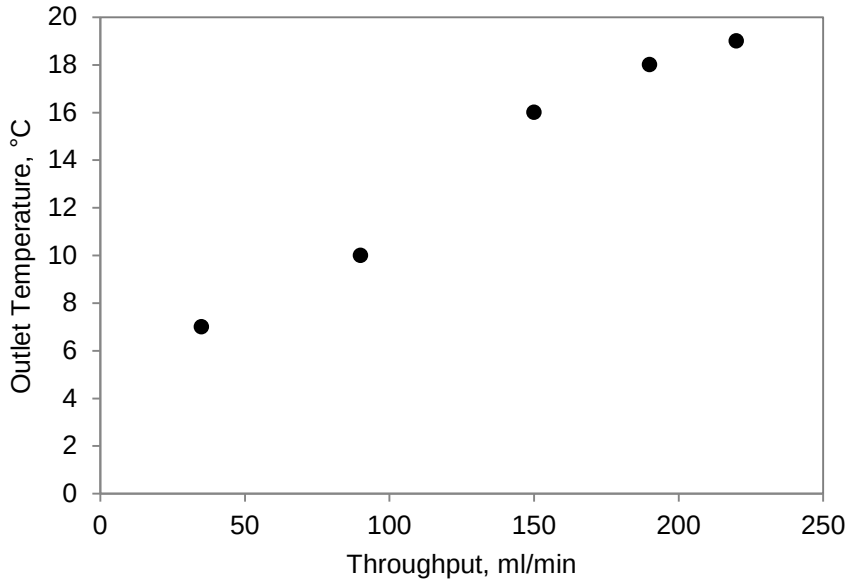

Figure 4.26: Plot showing the effect of throughput on the temperature of the fat system at the outlet of the A-unit.

The second type of viscosity profile found in Figure 4.25 is that of samples produced at a high rate of throughput (*i.e.* 220 ml/min). At low shear rates (< ~ 5 s^{-1}) these samples behave in a rheopectic manner and are similar to samples produced at high coolant temperatures in section 4.3, Figure 4.19. Application of shear at low shear rates seems to cause these samples to undergo structure formation resulting in an increased viscosity at the same shear rate in the ramp-down section of the experiment. At higher shear rates (> ~ 5 s^{-1}) however the behaviour of these samples is similar to the first type of viscosity profile; signs of structural deformation are detected as a reduction in viscosity is observed during the ramp-down of the experiment.

The third viscosity profile observed in Figure 4.25 is that of samples produced at 190 ml/min. These samples show no real thixotropic or rheopectic behaviour at shear rates of lower than ~ 1 s^{-1}. However at shear rates greater than 1 s^{-1} these samples behave in a similar fashion to those produced at lower throughput rates. At higher shear rates these samples show structural deformation as the results of the ramp-up and ramp-down of such systems are not the same. These systems, however, recover some of their lost structure at lower shear rates as no significant difference is observed between their viscosity values during the ramp-up and ramp-down sections of the experiment at lower shear rates. The effects of throughput on the elastic and viscous moduli of the fat systems are illustrated in Figure 4.27.

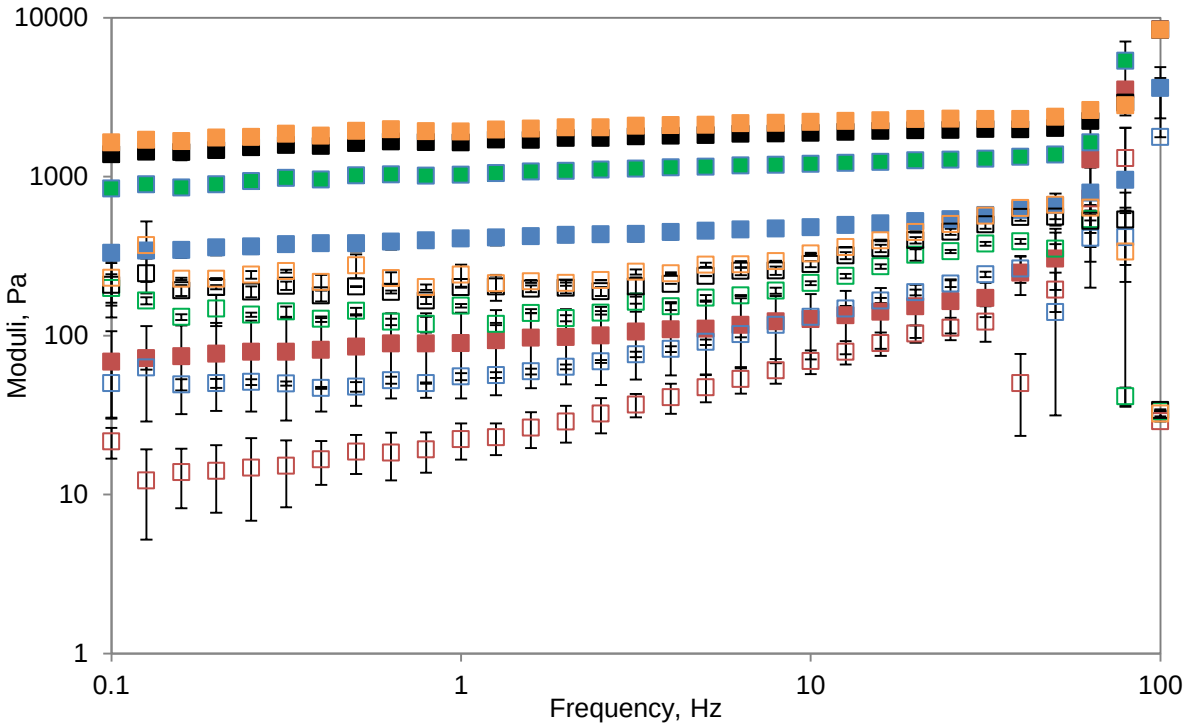

Figure 4.27: Plot of G' and G" against frequency for samples produced at various throughput rates. (■) Represents G' of samples produced at 220 ml/min; (□) Represents G'' of samples produced at 220 ml/min; (■) Represents G' of samples produced at 190 ml/min; (□) Represents G'' of samples produced at 190 ml/min; (■) Represents G' of samples produced at 150 ml/min; (□) Represents G'' of samples produced at 150 ml/min; (■) Represents G' of samples produced at 90 ml/min; (□) Represents G'' of samples produced at 90 ml/min; (■) Represents G' of samples produced at 35 ml/min; (□) Represents G'' of samples produced at 35 ml/min.

The effect of throughput on the viscous and elastic moduli of the fat systems is similar to that of coolant temperature as previously discussed in section 4.3. Figure 4.27 shows a general increase in the values of G' and G'' with increasing frequency, however this increase was greater for the viscous moduli. All samples were found to be solid-like across the frequency range as the values of G' were higher than those of G''. At the higher end of the frequency range the systems became more erratic and their moduli more irregular. It is also observed from Figure 4.27 that the G' and G'' moduli increase in value as a result of decreasing rate of throughput. However decreasing the throughput at higher values has a greater influence on the G' and G'', when compared to decreasing the throughput while already at lower values. This effect has been shown in Table 4.1. For instance decreasing the throughput from 150 ml/min to 90 ml/min results in a change in G' of 602 Pa (at 0.4 Hz); whereas decreasing the moduli from 90 ml/min to 35 ml/min results in an increase in G' of 247 Pa at the same frequency.

Table 4.1: Effect of change of throughput on the G' and G'' values at 0.4 Hz

	Difference		
Decrease in throughput, ml/min	**in rate, ml/min**	**in G', Pa**	**in G'', Pa**
190 to 150	40	577	80
150 to 90	60	602	52
90 to 35	55	247	38

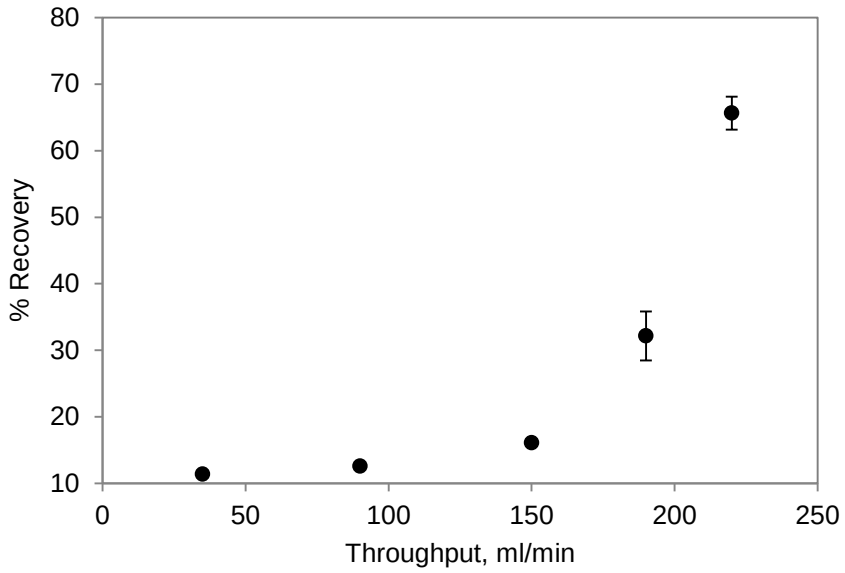

Figure 4.28: Plot of % recovery of the fat systems as a function of throughput.

Figure 4.28 shows the results of the hysteresis loop experiments carried out on samples produced at various throughputs. The results of this experiment are an indication of the ability of different systems to recover their structure. The general trend observed in Figure 4.28 is very similar to that of the effect of coolant temperature on the % recovery of fat systems, section 4.3. It is seen that increasing the throughput leads to an increase in the ability of the systems to recover their structure during the time frame of the experiment. The effect of the coolant temperature on the temperature at which the peak of the melting profile occurs is shown in Figure 4.29.

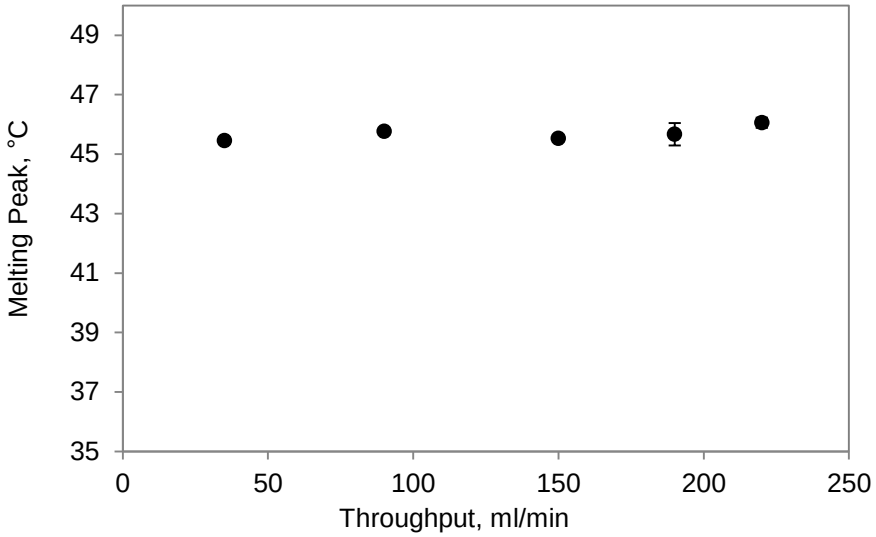

Figure 4.29: Graph of Melting peak (°C) against A-unit's Throughput (ml/min).

As illustrated by Figure 4.29 once again no difference in the melting peak of the fat systems (*i.e.* approximately 46 °C) is observed as a result of varying the throughput during production. It can therefore be assumed that varying the throughput of the A-unit does not result in the production of samples with different major polymorphic forms. This is similar to the results previously seen for the studies on the effects of mixing speed and coolant temperature on the melting behaviour of the fat systems.

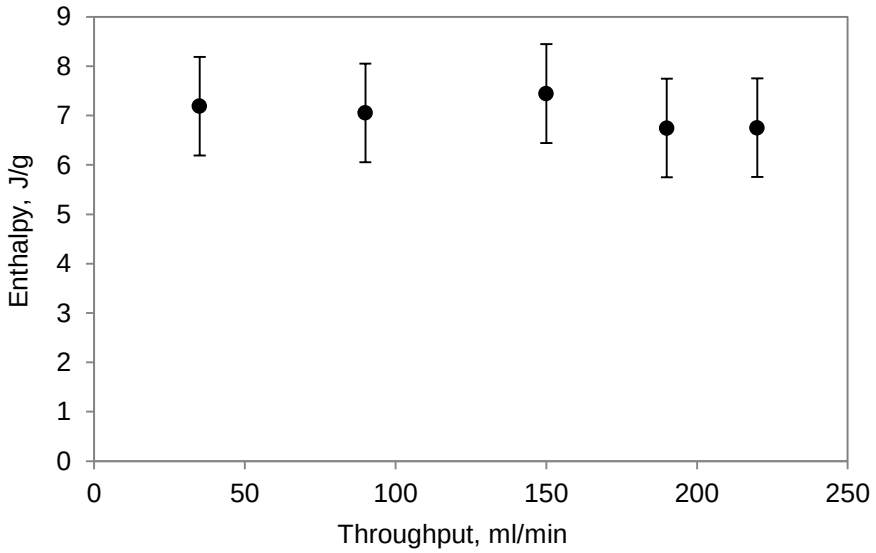

Figure 4.30: Plot of Enthalpy (J/g) of melting profiles against the Throughput (ml/min) of the A-unit.

Finally, Figure 4.30 illustrates how altering the throughput of the A-unit during production alters the enthalpy of fusion of the fat systems produced. As before, no difference in the enthalpies of fusion of samples produced at different rates of throughput is observed (i.*e.* approximately 7 J/g), see Figure 4.30; indicating that all samples contain the same amount of fat crystals.

5. CONCLUSIONS AND FUTURE WORK

5.1. Conclusions

Results obtained from the study looking into the effects of solid fat composition in a fat system provide an insight into their effects on the microstructure and thus the physical properties of fat crystal networks. It was observed that increasing the amount of solid fat gives rise to the formation of systems with higher viscosities. This is because a higher proportion of samples form crystals; this also shifts the maximum melting temperature and the crystallisation onset towards higher temperatures. This change to the microstructure also results in an increase in the fractal dimension of the system, which indicates an increase in the complexity of the microstructure. It was also observed that increasing the temperature results in a decrease in the viscosity of the system as the fat crystal network begins to melt and disintegrate. It was also established that all fat systems containing hydrogenated palm kernel oil were shear thinning and thixotropic.

The mixing speed of the A-unit was found to affect the microstructure of the systems as increasing the mixing speed during production resulted in the formation of fat networks with slightly higher values of elastic and viscous moduli. Results obtained from this study show no observed difference in viscosity, structural recovery, and melting behaviour of samples as a result of varying the mixing speed in a certain range (400 – 1500rpm, which is the maximum range of the A-unit).

The coolant temperature was found to have significant effects on the viscosity, moduli and the structural recovery of the fat systems. Producing fat systems at lower coolant temperatures resulted in more viscous and solid-like samples which are more thixotropic; this goes hand in hand with the literature as nucleation rate is partly governed by

temperature (Mullin, 2001). The reason for the changes observed is the formation of a stronger network of interconnected crystals possibly with different sizes and shapes; as lower coolant temperatures result in higher cooling rates which in turn control the size of the crystals being formed.

The effects of the throughput of the production system on the properties of the fat systems were found to be similar to those of the coolant temperature. Increasing the throughput leads to the production of fat systems with lower viscosities and lower elastic and viscous moduli, which did not undergo structural deformation and in some cases formed structure as a result of application of shear. This is because increasing the throughput decreases the time the melted fat mixture is in contact with the crystalliser walls and thus less crystallisation occurs at the walls of the heat exchanger and more occurs in the bulk of the mixture; giving rise to fat crystal networks with different properties. Similar to mixing speed, varying the coolant temperature and the throughput of the A-unit did not affect the melting behaviour (melting peak and enthalpy) of fat systems produced as their values were always ~ 46 °C and ~ 7 J/g respectively. This indicates the crystals present were of the same polymorphic form and that the fat systems contained the same amount of crystals.

In terms of industrial relevance the findings of this thesis could be used to alter the physical properties of model fat systems through processing conditions. This information can be used to produce two fat systems which behave in the same way, but have different solid fat levels. For example the residence time of a system containing a certain amount of high-melting fat can be controlled using the A-unit to provide the required amount of crystallisation and can be used to produce fat systems which differ in their physical properties.

5.2. Future Work

In the immediate future a deeper understanding of how formulation and processing conditions affect the microstructure of the fat network is required. Particularly in respect to how the solid fat content (SFC) values, and the morphologies of the crystals and crystal clusters present in the fat systems are affected, and how this affects the material properties of the crystal network. Pulsed nuclear magnetic resonance (pNMR) and scanning/transmission electron microscopy (SEM/TEM) can be used to investigate these effects.

The next step would be to use different production methods to understand how we can alter the behaviour of fat systems by varying the formulation approaches/techniques. This may include looking into ways of affecting the fat phase by introducing gelling agents, or methods to control crystallisation (such as seeding, shell formation, etc.). Since the overall aim of the project is to reduce the amount of saturated fat in baked products, it is important to investigate the effects of different fat systems on baked goods. Investigation into how the different fat systems interact with other ingredients in a bakery formulation, and how to optimise such interactions, will need to be conducted and an ideal fat formulation identified. Mechanical testing, such as texture profile analysis (TPA), can be used to study the effect on products.

Finally the effects of the microstructured fats on the organoleptic properties of the final baked product need to be studied and compared to a reference. This can be achieved through the use of sensory panels, which can also be used to establish relationships between the sensory and physical parameters previously obtained through mechanical testing.

6. APPENDIX

Melting profiles for samples produced at various processing conditions are shown here. No significant difference in the melting profiles is observed. Figures A.1, A.2, and A.3 represent the typical melting profiles observed for samples produced at different mixing speeds, coolant temperatures, and throughputs.

6.1. Effect of Mixing Speed on Melting Profile

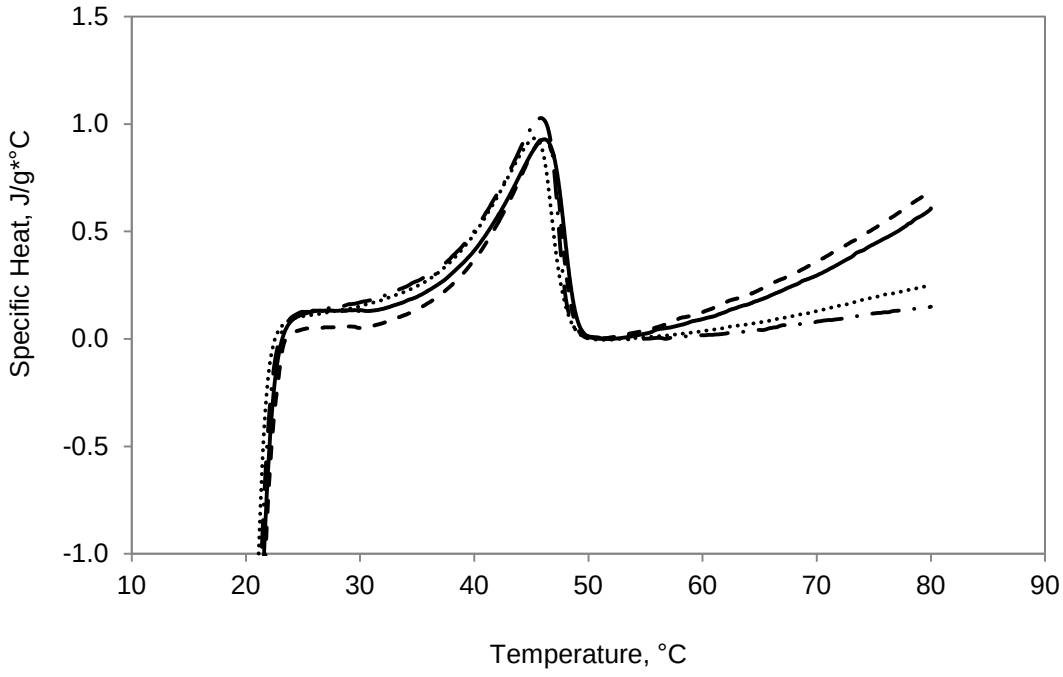

Figure A.1: Melting profiles of samples produced at various A-unit mixing speeds. (—) Represents samples produced at 1500 rpm; (···) Represents samples produced at 1200 rpm; (– –) Represents samples produced at 800 rpm; (– · –) Represents samples produced at 400 rpm.

6.2. Effect of Coolant Temperature on Melting Profile

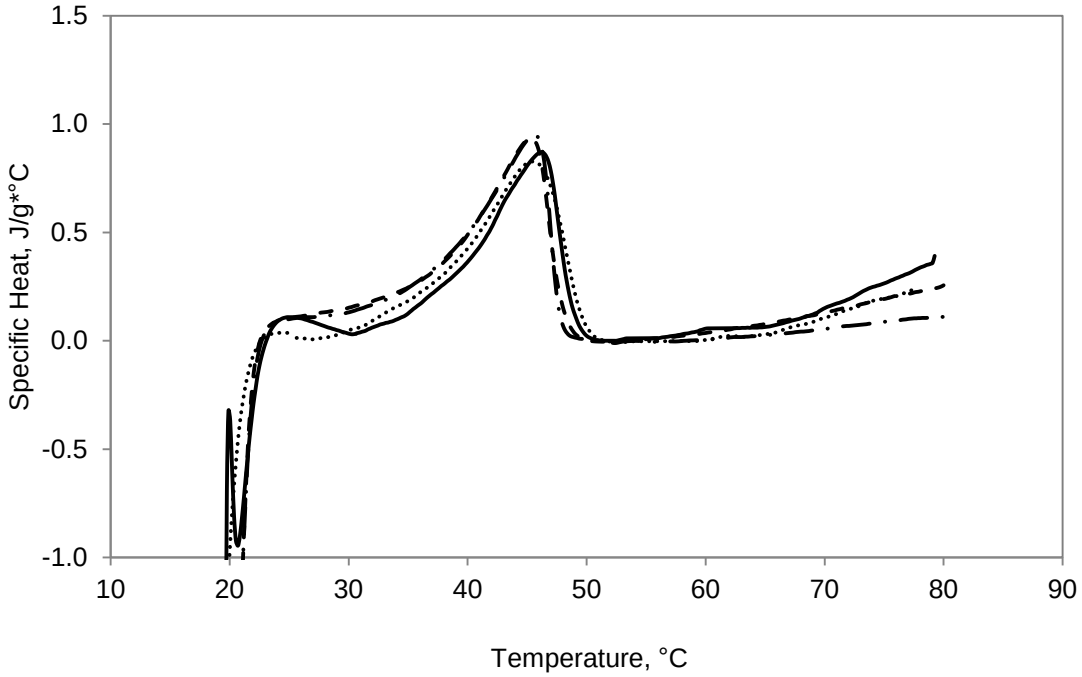

Figure A.2: Melting profiles of samples produced at various coolant temperatures. (—) Represents samples produced at 15 °C; (···) Represents samples produced at 10 °C; (– –) Represents samples produced at 5 °C; (– · –) Represents samples produced at 2 °C.

6.3. Effect of Throughput on Melting Profile

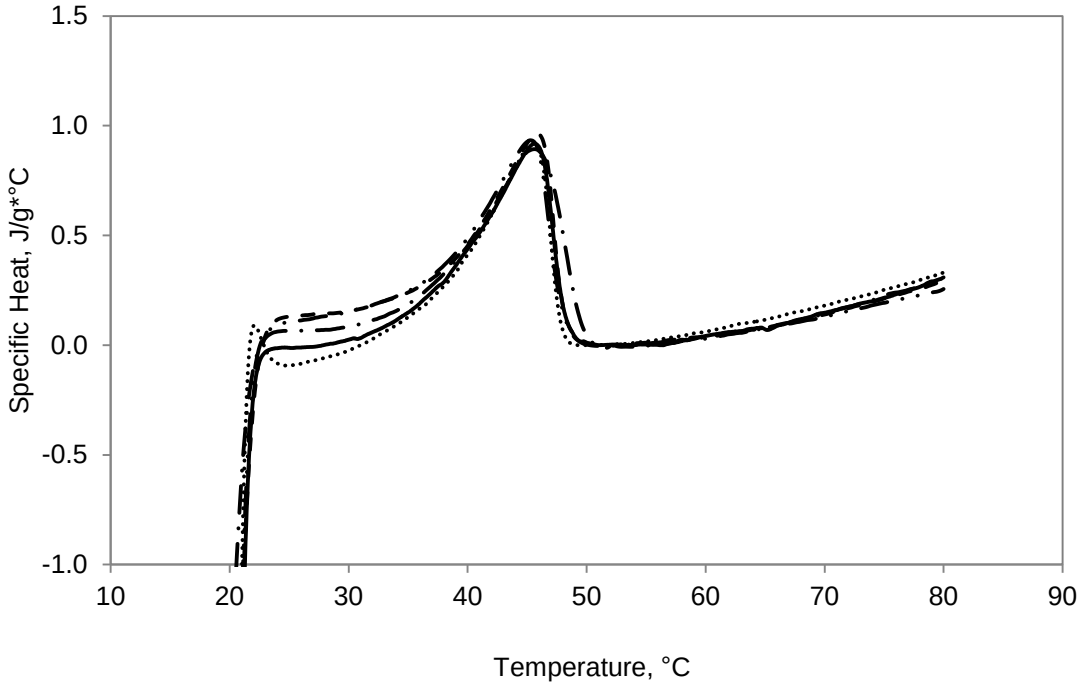

Figure A.3: Melting profiles of samples produced at various Throughput rates. (—) Represents samples produced at 220 ml/min; (···) Represents samples produced at 190 ml/min; (— —) Represents samples produced at 150 ml/min; (— · —) Represents samples produced at 90 ml/min; (— · · —) Represents samples produced at 35 ml/min.

7. REFERENCES

ARISHIMA, T., SAGI, N., MORI, H. & SATO, K. 1991. Polymorphism of POS: I. occurrence and polymorphic transformation. *Journal of the American Oil Chemists Society,* 68**,** 710-715.

AVNIR, D., FARIN, D. & PFEIFER, P. 1985. Surface geometric irregularity of particulate materials: The fractal approach. *Journal of Colloid and Interface Science,* 103**,** 112-123.

AWAD, T. S., ROGERS, M. A. & MARANGONI, A. G. 2004. Scaling Behavior of the Elastic Modulus in Colloidal Networks of Fat Crystals. *The Journal of Physical Chemistry B,* 108**,** 171-179.

BARNES, H. A. 1997. Thixotropy — a review. *Journal of Non-Newtonian Fluid Mechanics,* 70**,** 1-33.

BECKETT, S. T. 2000. *The science of chocolate*, Royal Society of Chemistry.

BOLLIGER, S., BREITSCHUH, B., STRANZINGER, M., WAGNER, T. & WINDHAB, E. J. 1998. Comparison of precrystallization of chocolate. *Journal of Food Engineering,* 35**,** 281-297.

BOYD, N., STONE, J., VOGT, K., CONNELLY, B., MARTIN, L. & MINKIN, S. 2003. Dietary fat and breast cancer risk revisited: a meta-analysis of the published literature. *British Journal of Cancer,* 89**,** 1672 – 1685.

BRIGGS, J. L. & WANG, T. 2004. Influence of Shearing and Time on the Rheological Properties of Milk Chocolate During Tempering. *JAOCS, Journal of the American Oil Chemists' Society,* 81**,** 117-121.

BRITANNICA, E. 2013. Polymorphism. *Encyclopædia Britannica Online*. Encyclopædia Britannica Inc.

CDC 2011. OBESITY halting the epidemic by making health easier.

CORBIT, J. D. & GARBARY, D. J. 1995. Fractal Dimension as a Quantitative Measure of Complexity in Plant Development. *Proceedings: Biological Sciences,* 262**,** 1-6.

DE BRUIJNE, D. W. & BOT, A. 1999. Fabricated fat-based foods. *Food texture: measurement and perception***,** 185-227.

DEMAN, J. M. & BEERS, A. M. 1987. FAT CRYSTAL NETWORKS: STRUCTURE AND RHEOLOGICAL PROPERTIES. *Journal of Texture Studies,* 18**,** 303-318.

FSA. 2008. *Saturated Fat and Energy Intake Programme* [Online]. Food Standards Agency. Available: http://www.food.gov.uk/multimedia/pdfs/satfatprog.pdf.

GONZALEZ-GUTIERREZ, J. & SCANLON, M. G. 2012. Rheology and Mechanical Properties of Fats. *In:* MARANGONI, A. G. (ed.) *Structure-Function Analysis of Edible Fats.* AOCS Press.

GOV.UK 2013. Reducing obesity and improving diet. *In:* HEALTH, D. O. (ed.).

GUNSTONE, F. D. 2006. Modifying Lipids for Use in Food. Woodhead Publishing.

HADNAĐEV, M., HADNAĐEV, T. D., TORBICA, A., DOKIĆ, L., PAJIN, B. & KRSTONOŠIĆ, V. 2011. Rheological properties of maltodextrin based fat - reduced confectionery spread systems. *Procedia Food Science,* 1**,** 62-67.

HEERTJE, I., CORNELISSEN, J. & JURIAANSE, A. 1988. The effect of processing on some microstructural characteristics of fat spreads. *Food microstructure,* 7**,** 189-193.

HEERTJE, I., LEUNIS, M., VAN ZEYL, W. J. M. & BERENDS, E. 1987. Product microscopy of fatty products. *Food Microstructure,* 6**,** 1-8.

HERRERA, M. L. & HARTEL, R. W. 2000. Effect of processing conditions on physical properties of a milk fat model system: Microstructure. *Journal of the American Oil Chemists' Society,* 77**,** 1197-1205.

HIGAKI, K., KOYANO, T., HACHIYA, I., SATO, K. & SUZUKI, K. 2004. Rheological properties of β-fat gel made of binary mixtures of high-melting and low-melting fats. *Food Research International,* 37**,** 799-804.

HMSO 2002. The National Diet & Nutrition Survey: adults aged 19 to 64 years - Types and quantities of foods consumed.

HUNCHAREK, M. & KUPELNICK, B. 2001. Dietary Fat Intake and Risk of Epithelial Ovarian Cancer: A Meta-Analysis of 6,689 Subjects From 8 Observational Studies. *Nutrition and Cancer,* 40**,** 87-91.

ISEO 1999. *Food Fats and Oils,* Institute of Shortening and Edible Oils.

MACMILLAN, S. D., ROBERTS, K. J., ROSSI, A., WELLS, M. A., POLGREEN, M. C. & SMITH, I. H. 2002. In Situ Small Angle X-ray Scattering (SAXS) Studies of Polymorphism with the Associated Crystallization of Cocoa Butter Fat Using Shearing Conditions. *Crystal Growth & Design,* 2**,** 221-226.

MALEKY, F. & MARANGONI, A. G. 2008. Process development for continuous crystallization of fat under laminar shear. *Journal of Food Engineering,* 89**,** 399-407.

MANDELBROT, B. B. 1982. *The Fractal Geometry of Nature,* Henry Holt and Company.

MARANGONI, A. G. 2002. The nature of fractality in fat crystal networks. *Trends in Food Science & Technology,* 13**,** 37-47.

MARANGONI, A. G. & MCGAULEY, S. E. 2002. Relationship between Crystallization Behavior and Structure in Cocoa Butter. *Crystal Growth & Design,* 3**,** 95-108.

MARANGONI, A. G. & ROUSSEAU, D. 1996. Is plastic fat rheology governed by the fractal nature of the fat crystal network? *Journal of the American Oil Chemists' Society,* 73**,** 991-994.

MARANGONI, A. G. & ROUSSEAU, D. 1998a. The influence of chemical interesterification on physicochemical properties of complex fat systems 1. Melting and crystallization. *Journal of the American Oil Chemists' Society,* 75**,** 1265-1271.

MARANGONI, A. G. & ROUSSEAU, D. 1998b. The influence of chemical interesterification on the physicochemical properties of complex fat systems. 3. Rheology and fractality of the crystal network. *Journal of the American Oil Chemists' Society,* 75**,** 1633-1636.

MARTINI, S., AWAD, T. & MARANGONI, A. G. 2006. Structure and properties of fat crystal networks. *In:* GUNSTONE, F. D. (ed.) *Modifying Lipids for Use in Food.* Woodhead Publishing.

MASLOW, A. H. 1943. A theory of human motivation. *Psychological Review,* 50**,** 370-396.

MAX-NEEF, M., ELIZALDE, A. & HOPENHAYN, M. 1989. Human Scale Development: An Option for the Future. *Development Dialogue, published by the Dag Hammarskjöld Foundation,* 1**,** 33.

MAZZANTI, G., GUTHRIE, S. E., SIROTA, E. B., MARANGONI, A. G. & IDZIAK, S. H. J. 2003. Orientation and phase transitions of fat crystals under shear. *Crystal Growth and Design,* 3**,** 721-725.

MEWIS, J. & WAGNER, N. J. 2009. Thixotropy. *Advances in Colloid and Interface Science,* 147–148**,** 214-227.

MULLIN, J. W. 2001. Nucleation. *Crystallization.* Butterworth-Heinemann.

NARINE, S. S. & MARANGONI, A. G. 1999a. Fractal nature of fat crystal networks. *Physical Review E,* 59**,** 1908-1920.

NARINE, S. S. & MARANGONI, A. G. 1999b. Relating structure of fat crystal networks to mechanical properties: a review. *Food Research International,* 32**,** 227-248.

OGDEN, C. L., CARROLL, M. D., KIT, B. K. & FLEGAL, K. M. 2012. *Prevalence of obesity in the United States, 2009-2010,* US Department of Health and Human Services, Centers for Disease Control and Prevention, National Center for Health Statistics.

PHAN-THIEN, N. & SAFARI-ARDI, M. 1998. Linear viscoelastic properties of flour–water doughs at different water concentrations. *Journal of Non-Newtonian Fluid Mechanics,* 74**,** 137-150.

RENTON, A. 2010. They were supposed to have been banished from the shelves, but lethal fats are STILL lurking in your weekly shopping. *Daily Mail*.

ROUSSET, P. & RAPPAZ, M. 1996. Crystallization kinetics of the pure triacylglycerols glycerol-1,3-dipalmitate-2-oleate, glycerol-1-palmitate-2-oleate-3-stearate, and glycerol-1,3-distearate-2-oleate. *Journal of the American Oil Chemists' Society,* 73**,** 1051-1057.
SANGWAL, K. & SATO, K. 2012. Nucleation and Crystallisation Kinetics of Fats. *In:* MARANGONI, A. G. (ed.) *Structure-Function Analysis of Edible Fats.* AOCS Press.
SATO, K. 2001a. Crystallization and Solidification Properties of Lipids. *In:* WIDLAK, N., HARTEL, R. & SURESH, N. (eds.) *Crystallization and Solidification Properties of Lipids.* AOCS Press.
SATO, K. 2001b. Crystallization behaviour of fats and lipids — a review. *Chemical Engineering Science,* 56**,** 2255-2265.
SATO, K., ARISHIMA, T., WANG, Z. H., OJIMA, K., SAGI, N. & MORI, H. 1989. Polymorphism of POP and SOS: I. occurrence and polymorphic transformation. *Journal of the American Oil Chemists' Society,* 66**,** 664-674.
SHI, Y., LIANG, B. & HARTEL, R. W. 2005. Crystal morphology, microstructure, and textural properties of model lipid systems. *Journal of the American Oil Chemists' Society,* 82**,** 399-408.
SHIH, W.-H., SHIH, W. Y., KIM, S.-I., LIU, J. & AKSAY, I. A. 1990. Scaling behavior of the elastic properties of colloidal gels. *Physical Review A,* 42**,** 4772-4779.
SIKORSKI, Z. E. & SIKORSKA-WISNIEWSKA, G. 2006. The Role of Lipids in Food Quality. *In:* WILLIAMS, C. & BUTTRISS, J. (eds.) *Improving the Fat Content of Foods.* Woodhead Publishing.
SIRI-TARINO, P. W., SUN, Q., HU, F. B. & KRAUSS, R. M. 2010. Meta-analysis of prospective cohort studies evaluating the association of saturated fat with cardiovascular disease. *American Journal of Clinical Nutrition,* 91**,** 535-546.
STAPLEY, A. G. F., TEWKESBURY, H. & FRYER, P. J. 1999. The effects of shear and temperature history on the crystallization of chocolate. *Journal of the American Oil Chemists' Society,* 76**,** 677-685.
TALBOT, G. 2011. Reducing Saturated Fats in Foods. Woodhead Publishing.
TANG, D. & MARANGONI, A. 2006a. Computer simulation of fractal dimensions of fat crystal networks. *Journal of the American Oil Chemists' Society,* 83**,** 309-314.
TANG, D. & MARANGONI, A. 2006b. Microstructure and fractal analysis of fat crystal networks. *Journal of the American Oil Chemists' Society,* 83**,** 377-388.
TANG, D. & MARANGONI, A. G. 2006c. 3D fractal dimension of fat crystal networks. *Chemical Physics Letters,* 433**,** 248-252.
TRIANTAFILLOPOULOS, N. 1988. Measurement of Fluid Rheology and Interpretation of Rheograms. 2nd ed.: Kaltec Scientific, Inc.
VREEKER, R., HOEKSTRA, L. L., DEN BOER, D. C. & AGTEROF, W. G. M. 1992. The fractal nature of fat crystal networks. *Colloids and Surfaces,* 65**,** 185-189.
WINDHAB, E. J. 1999. New Developments in Crystallization Processing. *Journal of Thermal Analysis and Calorimetry,* 57**,** 171-180.
YANO, J. & SATO, K. 1999. FT–IR studies on polymorphism of fats: molecular structures and interactions. *Food Research International,* 32**,** 249-259.